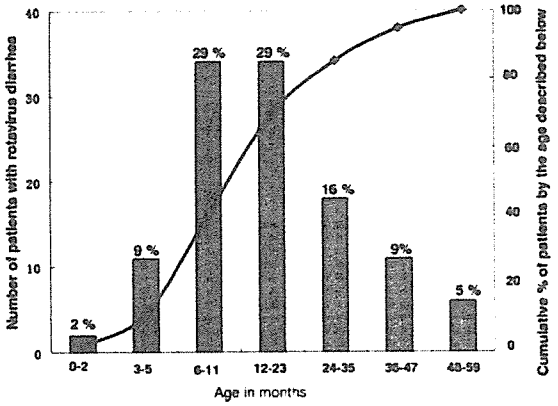

FIG. 1. The distribution of rotavirus diarrhea cases among children less than 5 years of age. Shaded columns represent the number of patients among the indicated age categories. The line indicated by "◆" shows the cumulative percentage of rotavirus-positive children by the indicated age.

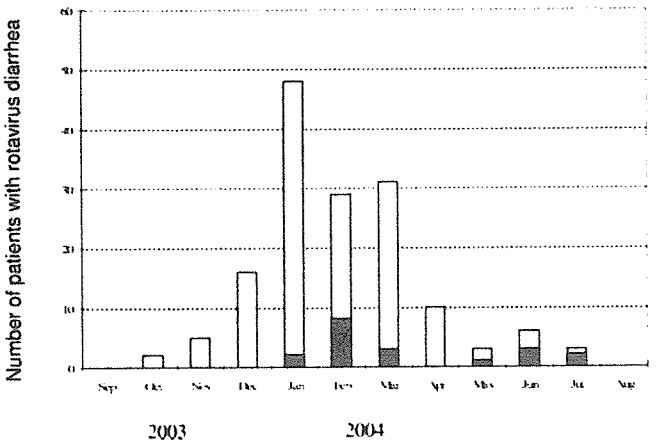

FIG. 2. Monthly occurrence of rotavirus diarrheal cases in children and adults in Nepal. The open column represents cases occurring in the group of patients less than 15 years of age, whereas the closed column represents cases occurring in the group of patients 15 years of age and older.

infections resulting in symptomatic disease. Based on a 4-year prospective study in a sentinel hospital in northern Japan, it was reported that rotavirus infection accounted for 10 to 15% of acute adult diarrhea cases encountered in the hospital (30). However, few studies have addressed the molecular epidemiology of rotavirus in adults, and knowledge in developing countries is completely lacking (1). Even though older children and adults may not escape rotavirus infections, it is conceivable that they have mounted certain levels of immunity against subsequent rotavirus infections based on previous exposures to rotavirus. Thus, characterization and comparison of rotaviruses circulating in different age groups may provide a key for understanding the spread of rotaviruses in the community.

Nepal is a landlocked mountainous country in Asia, with a very low per capita gross income. Available data show a high infant mortality rate (71 per 1,000 live births) (45) and a high child mortality rate due to diarrheal diseases (12). It is therefore likely that rotavirus is an important cause of childhood mortality. However, the literature on the epidemiology of rotavirus diarrhea in Nepal is scarce (26, 31, 39, 40), and molecular characterization of circulating strains has never been performed throughout a complete year.

The aim of this study was to determine the distribution of G and P serotypes and electropherotypes of rotaviruses circulating in children and adults in Nepal in order to examine if there is any emerging serotype or unusual strain in the region that may challenge the effectiveness of currently available rotavirus vaccines.

MATERIALS AND METHODS

Detection of rotavirus-positive stool specimens by ELISA. Stool specimens were collected from patients with acute diarrhea who were referred to the observation unit (outpatients, $n = 875$) and in the diarrheal ward (inpatients, $n = 30$) in Kanti Children's Hospital and from patients hospitalized for acute diarrhea in Sukra Raj Tropical and Infectious Disease Hospital (inpatients, $n = 410$), Kathmandu, Nepal, during a 1-year period between September 2003 and August 2004. A commercially available enzyme-linked immunosorbent assay (ELISA) kit (Rotaclone; Meridian Bioscience Inc., Cincinnati, OH) was used to detect group A rotavirus antigen. Rotavirus-positive specimens were partially purified by centrifugation through a 30% (wt/vol) sucrose cushion for 1 h at 50,000 rpm in a Beckman 100.2 rotor, and genomic RNAs were extracted with phenol chloroform and precipitated with ethanol.

Rotavirus G and P genotyping by reverse transcription-PCR (RT-PCR). G types were determined by using a method described previously by Gouvea et al. (17). For P types, the VP4 gene was amplified with con-2 and con-3 primers according to a method described previously by Gentsch et al. (15), and type-specific products were then obtained with specific typing primers described previously by Gunasena et al. (21). Those specimens that were amplified for their VP7 gene but that did not react with a single G-type-specific primer were recorded as G nontypeable. P nontypeable was defined in the same fashion.

Determination of G-nontypeable samples by RT-PCR based on deduced amino acids sequences in antigenic regions of VP7. For those samples that were G nontypeable by RT-PCR, a full-length VP7 gene was amplified with primers Beg9 and End9 using a QIAquick PCR purification kit (QIAGEN GmbH, Hilden, Germany) according to the manufacturer's instructions. Cycle sequencing was performed with an ABI PRISM BigDye Terminator v 3.1 cycle sequencing kit (Applied Biosystems, Foster City, CA), and products were loaded onto an ABI PRISM 3100 genetic analyzer (Applied Biosystems, Foster City, CA). G types were determined by a comparison of deduced amino acid sequences of antigenic regions A, B, and C of the VP7 protein (14) with reference strains.

Polyacrylamide gel electrophoresis of rotavirus genomic RNA. Rotavirus genomic RNAs were separated on a 10% polyacrylamide gel by electrophoresis for 16 h at a constant current of 8 mA per gel in a Laemmli buffer system using an SE600 Ruby gel apparatus (GE Healthcare Bioscience [formerly Amersham Biosciences], Piscataway, NJ) as described previously (25, 28). Electropherotypes were determined by comparisons of the individual RNA migration patterns of genome segments on the gel. Each electropherotype was designated E1, E2, E3, etc.

RESULTS

Epidemiologic features of rotavirus diarrhea in Nepal. Of 1,315 stool specimens collected from patients with acute diarrhea, rotavirus was detected in 153 (12%) specimens by ELISA. Rotavirus was detected in 116 (17%) of 666 specimens collected from patients under 5 years of age, in 18 (7%) of 260 of patients 5 to 14 years of age, and in 19 (5%) of 385 of patients 15 years of age or older. When the distribution of cases among patients under 5 years of age was examined, 68% occurred in those between 3 months and 23 months of age, while only 2% occurred in the first 3 months of life (Fig. 1).

There was seasonal variation in the occurrence of rotavirus diarrhea, with peaks in January and March and no cases in August and September (Fig. 2). Thus, rotavirus diarrhea was

TABLE 1. Comparison of amino acids sequences in antigenic regions A, B, and C of the VP7 protein between Nepali strains and reference G12 strains or the reference G11 strain[a]

Strain	Antigenic region of VP7		
	A (aa 87–96)	B (aa 145–150)	C (aa 211–223)
Nepali G12 strains	SSVTTEITDP	QNSLAL	DVTTFEEVANAEK
CP1030	----------	------	-------------
CP727	----------	------	-------------
ISO5	----------	------	-------------
ISO2	----------	------	-------------
ISO1	----------	------	-------------
T152	----------	------	-------------
Se585	----------	------	-------------
L26	N---------	------	--A----------
Nepali G11 strain	NEAATQIADD	DGNSQL	DPTTFEEVASAEK
Dhaka 6	----------	------	-------I-----
A253	R---------	------	----------T
YM	H---------	------	-------------

[a] Shown are G12 strains (29 samples) and reference G12 strains. Nepali G11 strain and reference G11 strains of human (Dhaka 6) and porcine origin are also shown. aa, amino acids.

most prevalent in the dry season in Nepal. However, this seasonal pattern was less marked in patients with rotavirus diarrhea who were 15 years of age and older, and cases in this age group accounted for 46% of rotavirus cases that occurred during the rainy season (from May to July) (Fig. 2).

The VP7 genes were successfully amplified in 142 (93%) of 153 rotavirus-positive specimens with RT-PCR. However, of these 142 samples, 30 were not typed with primers specific for G1 to G4, G8, or G9. When such VP7 amplicons were sequenced, it was found that 29 samples had completely identical amino acid sequences in antigenic regions A, B, and C of VP7. These 29 VP7 sequences were identified as G12 because they were identical to the amino acid sequences of reference G12 strains Se585, T152, ISO1, ISO2, ISO5, CP727, and CP1030 in antigenic regions A, B, and C (Table 1). The one remaining sample was typed as G11 because it had 100% amino acid sequence identity in antigenic regions A and B and 92% amino acid sequence identity in antigenic region C with strain Dhaka 6, the first human G11 strain available in the database (Table 1). Thus, of 153 rotavirus-positive specimens, 109 (77%) were typed as G1, 3 (2.1%) were typed as G2, 30 (20%) were typed as G12, and 1 (0.7%) was typed as G11 (Table 2).

For P types, 80% of the specimens were typed as P[8], 13% were typed as P[6], and 4.9% were nontypeable. When G and P types were combined, the majority (70%) of the specimens

TABLE 2. Distribution G and P types according to age categories

G and P type	No. of rotavirus-positive specimens (%) for age group:			
	<5 yr (n = 112)	5–14 yr (n = 17)	>15 yr (n = 13)	All (n = 142)
G1P[8]	78 (70)	13 (76)	9 (69)	100 (71)
G1P[6]	3 (3)	0 (0)	0 (0)	3 (2)
G1PNT[a]	5 (4)	0 (0)	1 (8)	6 (4)
G2P[4]	1 (1)	2 (12)	0 (0)	3 (2)
G12P[8]	10 (9)	0 (0)	3 (23)	13 (9)
G12P[6]	14 (12)	2 (12)	0 (0)	16 (11)
G11P[25]	1 (1)	0 (0)	0 (0)	1 (1)

[a] NT, nontypeable.

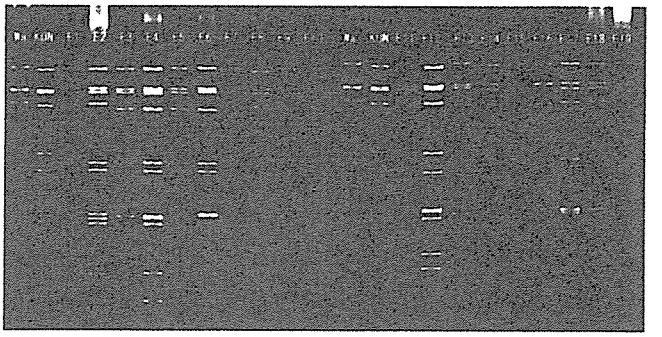

FIG. 3. Electropherotypes of rotavirus strains identified in Nepal during a 1-year period between September 2003 and August 2004. Electropherotypes named E3, E7, and E9 were codominant during the survey period. E1 and E18 viruses, both of which bear a G12P[6] specificity, look very similar on this panel, but it was observed in the original photograph as well as on another gel that segments 7 and 8 of E18 were clearly separated, whereas they were hardly so in E1. In addition, E3 and E4, both of which bear a G1P[8] specificity, look similar, but segments 7 and 8 were separated with a clear space between them when the genomic RNA was loaded slightly less on the gel (data not shown), thereby allocating a electropherotype number different from E3 whose segments 7 and 8 comigrated.

were G1P[8], while 20% were G12 with either P[6] or P[8] (Table 2). The P type of the G11 rotavirus was initially undetermined, but it was later typed as P[25] based on the result of the partial VP8* sequence. It was notable that the predominance of G1P[8] was observed for all three age groups, including older children and adults (Table 2). G12 strains were also found in all three age groups. On the other hand, P[6] was detected only in patients younger than 15 years of age (Table 2).

Molecular epidemiological analysis based on the comparison of electropherotypes and G and P types. Of 153 rotavirus-positive specimens analyzed by polyacrylamide gel electrophoresis, all 11 segments of genomic RNA were visualized in 57 (37%) specimens, which were classified into 19 electropherotypes (Fig. 3). The percentages of successful visualization of all 11 bands on the gel were different among the age groups, with 38% (44/116) in patients less than 5 years of age, 44% (8/18) in patients between 5 and 14 years of age, and 26% (5/19) in patients 15 years of age and older. This may suggest that less virus shedding occurred in the older age group, although the difference was not statistically significant. There were three codominant electropherotypes, named E3, E7, and E9, appearing in 11 (19%), 10 (18%), and 12 (21%) specimens, respectively (Table 3). No infection with more than one rotavirus strain was detected by RNA polyacrylamide gel electrophoresis. While this observation was unexpected, it does not entirely exclude the possibility of mixed infections, because the demonstration of more than 11 bands on the gel is an insensitive method of detecting mixed infections of more than one strain of rotavirus. Interestingly, there was one specimen that contained RNA patterns characteristic of reovirus as well as rotavirus (E11 in Fig. 3).

Each electropherotype corresponded to a single combination of G and P types, with an exception in which one specimen carrying E9 was typed as P nontypeable (Table 3). On the other hand, multiple electropherotypes existed within a single

TABLE 3. Rotavirus electropherotypes and G and P types according to age categories[a]

Electropherotype	G type	P type	No. of specimens for age group:			
			<5 yr	5–14 yr	>15 yr	All
E2	1	[8]	2	2		4
E3	1	[8]	6	4	1	11
E4	1	[8]	1			1
E7	1	[8]	8		2	10
E9	1	[8]	10	1		12
	1	NT	1			
E11	1	[8]	1			1
E13	1	[8]	1			1
E14	1	[8]	2			2
E19	1	[8]			*1*	*1*
E8	2	[4]	1			1
E12	2	[4]		*1*		*1*
E1	12	[6]	2			2
E15	12	[6]	1			1
E17	12	[6]	1			1
E18	12	[6]	1			1
E5	12	[8]	3			3
E6	12	[8]	1		1	2
E10	12	[8]	1			1
E16	11	[25]	1			1
Total			44	8	5	57

[a] Electropherotypes found in both the younger age group (under 5 years of age) and the older age groups (5 years of age and older) are underlined. Electropherotypes found only in the older age group are shown in italics. NT, nontypeable.

combination of G and P types (Table 3). Three codominant electropherotypes belonged to G1P[8], except one specimen that was G1P nontypeable, as mentioned above. All strains except G2P[4] carried a long RNA pattern, while all G2P[4] strains carried a short RNA pattern.

There was cocirculation of rotavirus strains with diverse electropherotypes over the 5-month period from December to April (Table 4). It was observed that despite the presence of many electropherotypes, there were not many different electropherotypes that were seen concurrently at any given period lasting more than 1 month. As to codominant strains, electropherotype E9 persisted the longest, for a 5-month period from January to May, followed by electropherotypes E3 and E7, which persisted during the same 4-months period, from December to March. Cocirculation of these three codominant strains was restricted in the period between January and March, which was the peak rotavirus season in Nepal. It deserves mention that the rotavirus strain bearing electropherotype E2 persisted the longest in the community, for at least 6 months, from October to March, although it never became dominant in the frequency of detection.

The distribution of electropherotypes in the three age groups is shown in Table 3. There were 17 electropherotypes in patients less than 5 years of age, 4 types in patients 5 to 14 years of age, and 4 types in patients 15 years of age or older. While the three codominant strains carrying electropherotypes E3, E7, and E9 had genotype G1P[8], their distribution among different age groups was different, and their frequency of detection was not necessarily proportionate to the number of rotavirus-positive specimens in each age group (Table 3). For example, electropherotype E9 seemed to be found more frequently in patients less than 5 years of age than in other age groups, and it was not found in patients 15 years of age and older. On the other hand, electropherotype E3 seemed to be disproportionately found in the older age groups.

When the two older age groups were combined and the age groups were redefined as the younger age group (under 5 years

TABLE 4. Monthly distribution of electropherotypes

Genotype	Electropherotype	No. of specimens[a]											
		Sept.	Oct.	Nov.	Dec.	Jan.	Feb.	Mar.	Apr.	May	June	July	Aug.
G1 codominant	E3				3	4	3	1					
	E7				1	6		3					
	E9					1	2	7	1	1			
G1 other than codominant	E2		1			2		1					
	E4			1									
	E11					1							
	E13						1						
	E14						2						
	E19										1		
G2	E8					1							
	E12					1							
G12P[6]	E1		1		1								
	E6				1		1						
	E15								1				
	E17								1				
	E18										1		
G12P[8]	E5				2	1							
	E10					1							
G11P[25]	E16								1				

[a] The numbers of patients in the peak month of codominant electropherotypes are underlined.

of age) and the older age group (5 years of age and older), five electropherotypes were found in both age groups, and they accounted for 68% of electropherotyped specimens. While 12 electropherotypes (28.5%) were found only in the younger age groups, there were only two electropherotypes (3.5%) unique to the older age group. A caveat here is, as stated above, that there was a smaller percentage (26%) of successful visualization of all 11 segments on the gel in the age group of 15 years and older than in the age groups of less than 5 years and 5 to 14 years (38 to 44%). Therefore, the possibility that the electropherotypic diversity in the older age group was more diverse than was observed in this study cannot be excluded.

DISCUSSION

Infants and young children under 2 years of age are most vulnerable to rotavirus infection that often results in severe diarrhea and dehydration, causing hospitalization and deaths. This age group has been the primary target of protection with rotavirus vaccines, and large-scale efficacy and safety trials of two major rotavirus vaccines have demonstrated the usefulness of these vaccines in developing countries (36, 46). The first dose of these vaccines are to be given between 6 and 12 weeks of age, and since the efficacy after the first dose alone has not been established, infants at this age period, i.e., those who are less than 3 months of age, will not be protected by the vaccine. Therefore, a detailed description of age groups that are most affected by rotavirus diarrhea will inform the optimum time for rotavirus vaccination. In Nepal, while only 2% of rotavirus diarrhea occurred before 3 months of age, the majority (68%) occurred between 3 and 23 months of age (Fig. 1). These data will support the introduction of rotavirus vaccines in Nepal according to the current schedule of the expanded program on immunization (6, 10, and 14 weeks).

While the majority of rotavirus diarrhea occurred in children less than 5 years of age, rotavirus diarrhea was not restricted to this age group; it occurred in 5 to 7% of diarrheal cases of older children and adults in Nepal. It bears repeating that patients aged 15 years and older were hospitalized patients, meaning that they had severe diarrhea and dehydration. Thus, this study confirmed and extended previous observations that rotavirus plays an important etiological role in acute diarrhea in older children and adults (1, 30).

The majority (73%) of the genotypes of rotavirus strains recovered from older children and adults were G1P[8], the relative frequency of which was almost identical to that of this genotype among children less than 5 years of age (70%) (Table 2). This observation may be in contrast to data from many previous reports in which rotavirus gastroenteritis outbreaks affecting older children and adults were attributed to infection with G2P[4] strains (18, 27). When G1P[8] rotaviruses found in different age groups were further analyzed by electropherotypes, it appeared that the detection of one codominant strain, E9, deviated toward the younger age group, whereas the detection of the other codominant strain, E3, deviated toward the older age group (Table 3). Thus, a hypothesis can be postulated that there are some antigenic differences even within the same G1P[8] strains that may affect the immunity conferred by prior rotavirus infections. However, the existence of such differences in the induction of protective immunity has not been systematically explored, except in the case of genotype-specific neutralization profiles within G9 rotaviruses (22).

Regarding the practical significance of antigenic differences accumulated over time on the VP7 protein, many previous vaccine trails provide evidence that the immunity conferred by an older G1 strain gave good clinical protection against severe diarrhea caused by more recent G1 strains circulating at the time of clinical trials. For example, (i) the G1 component of a tetravalent rhesus-human reassortant rotavirus vaccine (i.e., the VP7 of strain D isolated in the United States in 1974) (47) provided 88% protection against severe diarrhea caused by prevailing G1 viruses during a phase 3 clinical trial in 1994 to 1995 in Venezuela (33) (i.e., the 1974 G1 virus versus the G1 virus from 1994 to 1995); (ii) a G1 monovalent vaccine (Rotarix) derived from strain 89-12, isolated in the United States in 1988 (2), gave 90.8% protection against severe diarrhea caused by prevailing G1 viruses during a phase 3 clinical trial in 2003 to 2004 in 11 Latin American countries and Finland (36) (i.e., 1988 G1 virus versus the G1 virus from 2003 to 2004); and (iii) the G1 component of a pentavalent human-bovine vaccine (RotaTeq) (i.e., the VP7 of strain WI79 isolated in the United States in 1983) (6) provided 95.1% protection against severe diarrhea caused by prevailing G1 viruses during a phase 3 clinical trial from 2001 to 2004 in 11 countries (46) (i.e., 1983 G1 virus versus the G1 virus from 2001 to 2004).

A notable feature of the distribution of G and P genotypes in Nepal disclosed in this study was the greater dominance of G1P[8] and the emergence of G12 in combination with P[8] or P[6] as the second most common G type (20%). While the first human rotavirus strains carrying G12 were isolated in the Philippines in 1990 (44), G12 strains were reported in the United States (20) and Thailand (34) in 2002. There is an increasing number of G12 strains being reported in the literature, e.g., from India in 2003 (11), from Korea in 2002 to 2003 (24), from Japan in 2004 (41), and from Argentina in 2004 (5). Whereas these G12 strains were all from sporadic cases, there are more recent reports from India and Argentina showing that G12 strains are emerging as a significant proportion of rotaviruses causing diarrhea in children (4, 37). In Kolkata and Berhampur, India, from January 2003 to April 2005, the G1 genotype was the most predominant genotype (54%), followed by G2 (23%) and G12 (17%). The G12 viruses in that study were detected in association with P[4], P[8], and P[6] (37). Similarly, during the period between 1999 and 2003 in Buenos Aires, Argentina, the relative frequency of various G types was G4 (44.5%), followed by G1 (40.3%), G12 (6.7%), G9 (1.7%), and G2 (1.7%). In that study, G12 was found in association with either P[9] or a nontypeable P type (4). Taken together with our observation that G12 was found in combination with P[8] or P[6], it is tempting to speculate that G12 strains have evolved such that they are capable of spreading more frequently between humans by gaining the VP4 protein gene of the P[4], P[8], or P[6] specificity, which are common P genotypes found in human rotaviruses.

Of further interest was the detection of a G11 rotavirus in combination with P[25]. The human G11P[25] strain was first detected in Bangladesh in 2005 (35), so the detection in Nepal may imply that such unusual strains are on the increase in the Ganges region.

In the present study, P[6] strains were found only in the age

group under 15 years old, and its relative frequency was higher in Nepal than in other countries, except those in Africa (9, 10, 38, 43). Historically, P[6] strains were detected in asymptomatic neonates (23), but later studies established that rotaviruses with P[6] have also been recovered from children with diarrhea (19, 42). Continuous surveillance is needed to address the question of whether such P[6] rotaviruses will increase and spread to other age groups.

Genetic variability as revealed by the presence of multiple electropherotypes within the population is far greater in this study than, for example, in the study previously undertaken in Honjo, Japan, where the surveyed population was approximately 120,000 people (25). One major difference in the two settings was the size of the cohort in which rotavirus transmission was maintained. Kathmandu is the capital of Nepal with a population of approximately 1 million people with frequent communications with other areas of the country and thus has a much greater potential to maintain diverse strains of rotavirus during a limited time. This certainly favors the chance of coinfection with two or more strains, leading to the emergence of viral reassortants. Continuous rotavirus surveillance in Nepal is warranted to understand the mechanisms by which strain variability occurs under natural conditions.

ACKNOWLEDGMENTS

We thank Shouko Yamaguchi and Govinda Gurung for their excellent technical assistance. We also thank Kazuhiko Moji at the Institute of Tropical Medicine, Nagasaki University, for suggestions on statistical analysis.

This study was supported in part by the United States-Japan Cooperative Medical Science Program, a grant-in-aid for scientific research from the Japan Society for the Promotion of Science (grant number 16406016), and the Twenty-First Century Center of Excellence (COE) Program entitled Global Control Strategy of Tropical and Emerging Infectious Diseases. R.U. was formerly a postdoctoral fellow under the above-mentioned COE program.

REFERENCES

1. **Anderson, E. J., and S. G. Weber.** 2004. Rotavirus infection in adults. Lancet Infect. Dis. **4**:91–99.
2. **Bernstein, D. I., V. E. Smith, J. R. Sherwood, G. M. Schiff, D. S. Sander, D. DeFeudis, D. R. Spriggs, and R. L. Ward.** 1998. Safety and immunogenicity of live, attenuated human rotavirus vaccine 89-12. Vaccine **16**:381–387.
3. **Bresee, J., Z. Y. Fang, B. Wang, E. A. S. Nelson, J. Tam, Y. Sonetaro, S. A. Wilopo, P. Kilgore, J. S. Kim, J. O. Kang, W. S. Lan, C. L. Gaik, K. Moe, K. T. Chen, C. Jiraphongsa, Y. Pongsuwanna, N. V. Man, P. V. Tu, L. T. Luan, E. Hummelman, J. R. Gentsch, R. Glass, et al.** 2004. First report from the Asian Rotavirus Surveillance Network. Emerg. Infect. Dis. **10**:988–995.
4. **Castello, A. A., M. H. Argüelles, R. P. Rota, A. Olthoff, B. Jiang, R. L. Glass, J. R. Gentsch, and G. Glikmann.** 2006. Molecular epidemiology of group A rotavirus diarrhea among children in Buenos Aires, Argentina, from 1999 to 2003 and emergence of the infrequent genotype G12. J. Clin. Microbiol. **44**:2046–2050.
5. **Castello, A. A., M. L. Arvay, R. I. Glass, and J. Gentsch.** 2004. Rotavirus strain surveillance in Latin America: a review of the last nine years. Pediatr. Infect. Dis. J. **23**:S168–S172.
6. **Clark, H. F., F. E. Borian, K. Modesto, and S. A. Plotkin.** 1990. Serotype 1 reassortant of bovine rotavirus WC3, strain WI79-9, induces a polytypic antibody response in infants. Vaccine **8**:327–332.
7. **Clark, H. F., P. S. Offit, R. I. Glass, and R. L. Ward.** 2004. Rotavirus vaccines, p. 1327–1345. *In* S. A. Plotkin and W. A. Orenstein (ed.), Vaccines, 4th ed. Saunders, Philadelphia, Pa.
8. **Cunliffe, N. A., and O. Nakagomi.** 2005. A critical time for rotavirus vaccines: a review. Expert Rev. Vaccines **4**:521–532.
9. **Cunliffe, N. A., J. R. Gentsch, C. D. Kirkwood, J. S. Gondwe, W. Dove, O. Nakagomi, T. Nakagomi, Y. Hoshino, J. S. Bresee, R. I. Glass, M. E. Molyneux, and C. A. Hart.** 2000. Molecular and serologic characterization of novel serotype G8 human rotavirus strains detected in Blantyre, Malawi. Virology **274**:309–320.
10. **Cunliffe, N. A., J. S. Gondwe, S. M. Graham, B. D. Thindwa, W. Dove, R. L. Broadhead, M. E. Molyneux, and C. A. Hart.** 2001. Rotavirus strain diversity in Blantyre, Malawi, from 1997 to 1999. J. Clin. Microbiol. **39**:836–843.
11. **Das, S., V. Varghese, S. Chaudhury, P. Barman, S. Mahapatra, K. Kojima, S. K. Bhattacharya, T. Krishnan, R. K. Ratho, G. P. Chhotray, A. C. Phukan, N. Kobayashi, and T. N. Naik.** 2003. Emergence of novel human group A rotavirus G12 strains in India. J. Clin. Microbiol. **41**:2760–2762.
12. **Department of Health Services, Ministry of Health, His Majesty's Government of Nepal.** 2003. Control of diarhhoeal disease, p. 45–53. *In* Annual Report Department of Health Services 2058/59 (2001/2002). Department of Health Services, Ministry of Health, His Majesty's Government of Nepal, Kathmandu, Nepal.
13. **Dunn, S. J., R. L. Ward, M. M. McNeal, T. L. Cross, and H. B. Greenberg.** 1993. Identification of a new neutralization epitope on VP7 of human serotype 2 rotavirus and evidence for electropherotype difference caused by single nucleotide substitutions. Virology **197**:397–404.
14. **Dyall-Smith, M. L., I. Lazdins, G. W. Tregear, and I. H. Holmes.** 1986. Location of the major antigenic sites involved in rotavirus serotype-specific neutralization. Proc. Natl. Acad. Sci. USA **83**:3465–3468.
15. **Gentsch, J. R., R. I. Glass, P. Woods, V. Gouvea, M. Gorziglia, J. Flores, B. K. Das, and M. K. Bhan.** 1992. Identification of group A rotavirus gene 4 types by polymerase chain reaction. J. Clin. Microbiol. **30**:1365–1373.
16. **Gentsch, J. R., A. R. Laird, B. Bielfelt, D. D. Griffin, K. Bányai, M. Ramachandran, V. Jain, N. A. Cunliffe, O. Nakagomi, C. D. Kirkwood, T. K. Fischer, U. D. Parashar, J. S. Bresee, B. Jaing, and R. I. Glass.** 2005. Serotype diversity and reassortment between human and animal rotavirus strains: implications for rotavirus vaccine programs. J. Infect. Dis. **192**:S146–S159.
17. **Gouvea, V., R. I. Glass, P. Wood, K. Taniguchi, H. F. Clark, B. Forreter, and Z. Y. Fang.** 1990. Polymerase chain reaction amplification and typing of rotavirus nucleic acid from stool specimens. J. Clin. Microbiol. **28**:276–282.
18. **Griffin, D. D., M. Fletcher, M. E. Levy, M. Ching-Lee, R. Nogami, L. Edwards, H. Peters, L. Montague, J. R. Gentsch, and R. I. Glass.** 2002. Outbreaks of adult gastroenteritis traced to a single genotype of rotavirus. J. Infect. Dis. **185**:1502–1505.
19. **Griffin, D. D., C. D. Kirkwood, U. D. Parashar, P. A. Woods, J. S. Bresee, R. I. Glass, and J. R. Gentsh.** 2000. Surveillance of rotavirus strains in the United States: identification of unusual strains. J. Clin. Microbiol. **38**:2784–2787.
20. **Griffin, D. D., T. Nakagomi, Y. Hoshino, O. Nakagomi, C. D. Kirkwood, U. D. Parashar, R. I. Glass, J. R. Gentsch, and the National Rotavirus Surveillance System.** 2002. Characterization of nontypeable rotavirus strains from the United States: identification of a new rotavirus reassortant (P2A[6],G12) and rare P3[9] strains related to bovine rotaviruses. Virology **294**:256–269.
21. **Gunasena, S., O. Nakagomi, Y. Isegawa, E. Kaga, T. Nakagomi, A. D. Steele, J. Flores, and S. Ueda.** 1993. Relative frequency of VP4 gene alleles among human rotavirus recovered over a 10-year period (1982–1991) from Japanese children with diarrhea. J. Clin. Microbiol. **31**:2195–2197.
22. **Hoshino, Y., R. W. Jones, J. Ross, S. Honma, N. Santos, J. R. Gentsch, and A. Z. Kapikian.** 2004. Rotavirus serotype G9 strains belonging to VP7 gene phylogenetic sequence lineage 1 may be more suitable for serotype G9 vaccine candidates than those belonging to lineage 2 or 3. J. Virol. **78**:7795–7802.
23. **Hoshino, Y., R. G. Wyatt, J. Flores, K. Midthun, and A. Z. Kapikian.** 1985. Serotypic characterization of rotaviruses derived from asymptomatic human neonatal infections. J. Clin. Microbiol. **21**:425–430.
24. **Kang, J. O., P. Kilgore, J. S. Kim, B. Nyambat, J. Kim, H. S. Suh, Y. Yoon, S. Jang, C. Chang, S. Choi, M. N. Kim, J. Gentsch, J. Bresee, and R. Glass.** 2005. Molecular epidemiological profile of rotavirus in South Korea, July 2002 through June 2003: emergence of G4P[6] and G9P[8] strains. J. Infect. Dis. **192**:S57–S63.
25. **Koshimura, Y., T. Nakagomi, and O. Nakagomi.** 2000. The relative frequencies of G serotypes of rotaviruses recovered from hospitalized children with diarrhea: a 10-year survey (1987–1996) in Japan with a review of globally collected data. Microbiol. Immunol. **44**:499–510.
26. **Kurokawa, M., K. Ono, M. Nukina, M. Itoh, U. Thapa, and S. K. Rai.** 2004. Detection of diarrheagenic viruses from diarrheal fecal samples collected from children in Kathmandu, Nepal. Nepal Med. Coll. J. **6**:17–23.
27. **Mikami, T., T. Nakagomi, R. Tsutsui, K. Ishikawa, Y. Onodera, K. Arisawa, and O. Nakagomi.** 2004. An outbreak of gastroenteritis during school trip caused by serotype G2 group A rotavirus. J. Med. Virol. **73**:460–464.
28. **Nakagomi, T., K. Akatani, N. Ikegami, N. Katsushima, and O. Nakagomi.** 1988. Occurrence of changes in human rotavirus serotypes with concurrent changes in genomic RNA electropherotypes. J. Clin. Microbiol. **26**:2586–2592.
29. **Nakagomi, T., J. R. Gentsch, B. K. Das, R. Kumar, M. K. Bhan, R. I. Glass, and O. Nakagomi.** 2002. Molecular characterization of serotype G2 and G3 human rotavirus strains that have apparently identical electropherotype of the short RNA pattern. Arch. Virol. **147**:2187–2195.
30. **Nakajima, H., T. Nakagomi, T. Kamisawa, N. Sasaki, K. Muramoto, T. Mikami, H. Nara, and O. Nakagomi.** 2001. Winter seasonality and rotavirus diarrhoea in adults. Lancet **357**:1950.

31. **Ono, K., S. K. Rai, M. Chikahira, T. Fujimoto, H. Shibata, Y. Wada, H. Tsuji, Y. Oda, G. Rai, C. D. Shrestha, K. Masuda, H. G. Shrestha, T. Matsumura, H. Hotta, T. Kawamura, and S. Uga.** 2001. Seasonal distribution of enteropathogens detected from diarrheal stool and water samples collected in Kathmandu, Nepal. Southeast Asian J. Trop. Med. Public Health **32**:520–526.
32. **Parashar, U. D., E. G. Hummelman, J. S. Bresee, M. A. Miller, and R. I. Glass.** 2003. Global illness and deaths caused by rotavirus disease in children. Emerg. Infect. Dis. **9**:565–572.
33. **Perez-Schael, I., M. J. Guntinas, M. Perez, V. Pagone, A. M. Rojas, R. Gonzalez, W. Cunto, Y. Hoshino, and A. Z. Kapikian.** 1997. Efficacy of the rhesus rotavirus-based quadrivalent vaccine in infants and young children in Venezuela. N. Engl. J. Med. **337**:1181–1187.
34. **Pongsuwanna, Y., R. Guntapong, M. Chiwakul, R. Tacharoenmuang, N. Onvimala, M. Wakuda, N. Kobayashi, and K. Taniguchi.** 2002. Detection of a human rotavirus with G12 and P[9] specificity in Thailand. J. Clin. Microbiol. **40**:1390–1394.
35. **Rahman, M., J. Matthijnssens, S. Nahar, G. Podder, D. A. Sack, T. Azim, and M. Van Ranst.** 2005. Characterization of a novel P[25],G11 human group A rotavirus. J. Clin. Microbiol. **43**:3208–3212.
36. **Ruiz-Palacios, G. M., I. Perez-Schael, F. R. Velazquez, H. Abate, T. Breuer, S. C. Clemens, B. Cheuvart, F. Espinoza, P. Gillard, B. L. Innis, Y. Cervantes, A. C. Linhares, P. Lopez, M. Macias-Parra, E. Ortega-Barria, V. Richardson, D. M. Rivera-Medina, L. Rivera, B. Salinas, N. Pavia-Ruz, J. Salmeron, R. Ruttimann, J. C. Tinoco, P. Rubino, E. Nunez, M. L. Guerrero, J. P. Yarzabal, S. Damaso, N. Tornieporth, X. Saez-Llorens, R. F. Vergara, T. Vesikari, A. Bouckenooghe, R. Clemens, B. De Vos, and M. O'Ryan.** 2006. Safety and efficacy of an attenuated vaccine against severe rotavirus gastroenteritis. N. Engl. J. Med. **354**:11–22.
37. **Samajdar, S., V. Varghese, P. Barman, S. Ghosh, U. Mitra, P. Dutta, S. K. Bhattacharya, M. V. Narasimham, P. Panda, T. Krishnan, N. Kobayashi, and T. N. Naik.** 2006. Changing pattern of human group A rotaviruses: emergence of G12 as an important pathogen among children in eastern India. J. Clin. Virol. **36**:183–188.
38. **Santos, N., and Y. Hoshino.** 2005. Global distribution of rotavirus serotypes/genotypes and its implication for the development and its implementation of an effective rotavirus vaccine. Rev. Med. Virol. **15**:29–56.
39. **Sherchand, J. B., S. Larsson, B. J. Rana, H. Dixit, D. S. Bam, R. K. Adhikari, P. R. Sharma, M. K. Shrestha, and M. P. Shresta.** 1992. On the incidence of rotavirus and enteric adenovirus diarrhoea in children attending the outpatient department of Kanti Children's Hospital and general practitioners in the Kathmandu area. J. Nepalese Med. Assoc. **30**:149–153.
40. **Sherchand, J. B., and K. Haruki.** 2004. Rotavirus diarrhoea in children and animals of urban and rural Nepal. J. Nepal Health Res. Council **2**:5–8.
41. **Shinozaki, K., M. Okada, S. Nagashima, I. Kaiho, and K. Taniguchi.** 2004. Characterization of human rotavirus strains with G12 and P[9] detected in Japan. J. Med. Virol. **73**:612–616.
42. **Steele, A. D., M. C. van Niekerk, and M. J. Mphahlele.** 1995. Geographic distribution of human rotavirus VP4 genotypes and VP7 serotypes in five South African regions. J. Clin. Microbiol. **33**:1516–1519.
43. **Steele, A. D., and B. Ivanoff.** 2003. Rotavirus strains circulating in Africa during 1996–1999: emergence of G9 strains and P[6] strains. Vaccine **21**: 361–367.
44. **Taniguchi, K., T. Urasawa, N. Kobayashi, M. Gorziglia, and S. Urasawa.** 1990. Nucleotide sequence of VP4 and VP7 genes of human rotaviruses with subgroup I specificity and long RNA pattern: implication for new G serotype specificity. J. Virol. **64**:5640–5644.
45. **United Nations Population Fund.** 2004. Monitoring ICPD goals—selected indicators, p. 102–105. *In* W. A. Ryan (ed.), The state of world population 2004. United Nations Population Fund, New York, N.Y.
46. **Vesikari, T., D. O. Matson, P. Dennehy, P. Van Damme, M. Santosham, Z. Rodriguez, M. J. Dallas, J. F. Heyse, M. G. Goveia, S. B. Black, H. R. Shinefield, C. D. Christie, S. Ylital, R. F. Itzler, M. L. Cois, M. T. Onorato, B. A. Adeyi, G. S. Marshall, L. Gothefors, D. Campens, A. Karvonen, J. P. Watt, K. L. O'Brien, M. J. DiNubile, H. F. Clark, J. W. Boslego, P. A. Offit, and P. M. Heaton.** 2006. Safety and efficacy of a pentavalent human-bovine (WC3) reassortant rotavirus vaccine. N. Engl. J. Med. **354**:23–33.
47. **Wyatt, R. G., H. D. James, Jr., A. L. Pittman, Y. Hoshino, H. B. Greenberg, A. R. Kalica, J. Flores, and A. Z. Kapikian.** 1983. Direct isolation in cell culture of human rotaviruses and their characterization into four serotypes. J. Clin. Microbiol. **18**:310–317.

Journal of Medical Microbiology (2006), 55, 905–911 DOI 10.1099/jmm.0.46580-0

Helicobacter pylori-associated oxidant monochloramine induces reactivation of Epstein–Barr virus (EBV) in gastric epithelial cells latently infected with EBV

Junko Minoura-Etoh,[1] Kazuyo Gotoh,[1] Ryugo Sato,[2] Masao Ogata,[2] Naomi Kaku,[3] Toshio Fujioka[4] and Akira Nishizono[1]

Correspondence
Akira Nishizono
a24zono@med.oita-u.ac.jp

Microbiology[1], Second Internal Medicine[2], Oral-Maxillary Surgery[3] and General Medicine[4], Department of Infectious Diseases, Faculty of Medicine, Oita University, Oita, Japan

Received 16 February 2006
Accepted 14 March 2006

To investigate the possibility of an interaction between two ubiquitous human pathogens, *Helicobacter pylori* and Epstein–Barr virus (EBV), the effect of monochloramine (NH_2Cl), locally produced by *H. pylori* infection, on gastric epithelium latently infected with EBV was examined, by assessing the induction of EBV lytic infection. AGS cells harbouring latently infected EBV were used as the indicator of lytic change caused by NH_2Cl treatment. Lytic infection, determined by morphological change and EA-D antigen expression, occurred immediately after treatment with *in vitro*-synthesized NH_2Cl. Analysis of EBV infection in human gastric tissue revealed that out of 48 *H. pylori*-positive patients, 24 were positive for EBER-1, and 18 and 13 were positive for EBNA1 and LMP-1 antigen, respectively. The results suggest that *H. pylori*-associated NH_2Cl induces EBV lytic conversion in gastric epithelium latently infected with EBV.

INTRODUCTION

Chronic microbial infections induce malignant tumours in humans and animals. It is well known that *H. pylori* infection is closely associated with gastric mucosal atrophy, intestinal metaplasia and subsequent well-differentiated adenocarcinoma of the stomach via a cause–effect relationship between microbial infection and gastric carcinogenesis (Nomura *et al.*, 1991; Parsonnet *et al.*, 1991). Epstein–Barr virus (EBV) is a ubiquitous herpes virus that is well documented to be causally associated with various malignant tumours, including Burkitt's lymphoma, nasopharyngeal carcinoma, and B-cell lymphoma in immunodeficient individuals, and is also known to be an important aetiologic agent of gastric carcinoma, as is *H. pylori* (Rickinson & Kieff, 2001). Approximately 7 % of gastric carcinomas are reported to be monoclonal proliferations of gastric epithelial cells infected by EBV (Imai *et al.*, 1994), and lymphoepithelioma-like carcinoma of the stomach is the most prevalent phenotype in EBV-infected gastric carcinoma (Wu *et al.*, 2000). All EBV-carrying gastric carcinomas have been reported to have individual single clonotypes of EBV DNA, as determined by terminal repeat (TR) analysis and the presence of EBV-encoded small RNA1 (EBER-1) (Fukayama *et al.*, 1994).

Abbreviations: EBV, Epstein–Barr virus; FACS, fluorescence-activated cell sorting; FBS, fetal bovine serum; ISH, *in situ* hybridization; TPA, 12-*O*-tetradecanoylphorbol-13-acetate.

EBV preferentially infects B lymphocytes via the EBV receptor (CD21), and the major envelope protein of EBV gp350/220 is a ligand for CD21 (Kieff & Rickinson, 2001). Although EBV primarily infects the mucosal epithelium of the oropharynx, such epithelial cells do not possess CD21 molecules on their surface, unlike B cells (Janz *et al.*, 2000). The mechanisms of the primary viral infection of epithelium, especially gastric cells, are not understood. According to a recent report, EBV infections are detected in non-carcinoma gastric epithelium characterized by chronic atrophic gastritis accompanied by intestinal metaplasia (Yanai *et al.*, 1997). Whether such gastric epithelium latently infected with EBV functions as the progenitor of gastric carcinoma or as a producer of progeny virus is not understood. Although the EBV genome is latent in B cells and oropharyngeal/gastric epithelial cells in the carrier state, reactivation of the EBV genome occurs after various stimuli, whereby it enters into the viral lytic cycle (Kieff & Rickinson, 2001). A number of different stimuli or agents *in vitro* have been shown to trigger the switch from the latent infection state into the lytic infection. These include halogenated pyrimidines, nutrient starvation, phorbol esters, calcium ionophores, transforming growth factor beta 1 (TGF-β1), *n*-butyrate, histone deacetylase inhibitors, azacytidine, and cross-linking of surface immunoglobulin (Gradoville *et al.*, 2002). Of these lytic-infection-inducing stimuli, several are capable of leading to cell cycle arrest or cell death (Kudoh *et al.*, 2003).

H. pylori-colonized gastric mucosa is characterized by dominant accumulation of neutrophils and lymphocytes in the infected gastric mucosa; activated neutrophils generate $O_2^{\cdot-}$ and H_2O_2 (Morris & Nicholson,1987). Myeloperoxidase in neutrophils catalyses the oxidation of chloride by H_2O_2 to yield hypochlorous acid (HOCl). The interaction between *H. pylori*-derived NH_3 and HOCl produces monochloramine (NH_2Cl), which is reactive and toxic, and leads to gastric mucosal cell injury via destruction of DNA double strands and chromatin condensation because of its lipophilic properties and low molecular mass (Murakami *et al.*, 1995; Sato *et al.*, 1999; Suzuki *et al.*,1992). In addition, NH_2Cl is known to induce detachment of various types of cells (fibroblasts, epithelial cells and endothelial cells) from culture dishes, with concomitant cell shrinkage (Nakamura *et al.*, 1995).

Thus, both *H. pylori* and EBV infect the human stomach, and therefore may have a synergistic relationship or some other form of impact on each other. The aim of the present study was to examine whether *H. pylori* induces reactivation of the EBV lytic cycle in the human gastric epithelium which these two pathogens commonly colonize, via a cell damage process induced by NH_2Cl production.

METHODS

Cell culture. AGS-neo cells were transfected with recombinant EBV containing the neomycin resistance (Neo^r) gene at the BZLF1 site of EBV DNA, which is non-essential for infection and replication in AGS cells. The original AGS cell line was a gastric carcinoma cell line derived from a signet ring cell carcinoma of the stomach. This cell line was kindly provided by Professor K. Takada and Dr H. Yoshiyama, Hokkaido University School of Medicine (Yoshiyama *et al.*, 1997). Cells were subcultured twice a week (5×10^4 cells ml^{-1}) in F-12 (HAM) Nutrient Mixture medium (Gibco) supplemented with 10% (v/v) non-heat-inactivated fetal bovine serum (FBS) (Equitech-bio, ICN Pharmaceuticals), 100 U penicillin ml^{-1}, 100 μg streptomycin ml^{-1} and 500 μg geneticin ml^{-1}. B95-8 and Raji cells were cultured in RPMI1640 medium (Gibco) supplemented with 10% (v/v) heat-inactivated FBS, 100 U penicillin ml^{-1} and 100 μg streptomycin ml^{-1}.

Preparation of NH_2Cl *in vitro*. *In vitro* synthesis of NH_2Cl was carried out according to the method of Grisham *et al.* (1990). Briefly, NH_2Cl was synthesized by adding NaOCl to a solution of ammonium chloride in 0·05 M phosphate buffer (pH 8·0). The concentration of NH_2Cl was determined assuming a molar extinction coefficient of 429 at 242 nm.

Detection of EBV EA-D by Western blotting and immunofluorescence microscopy. Western blotting was performed as described previously (Sumie *et al.*, 2001). Briefly, the cell lysate was subjected to SDS-12·5% PAGE and the resolved proteins were electroblotted onto a PVDF membrane. The blotted membrane was reacted with 1:5000-diluted mouse anti-EBV EA-D-p52/50 monoclonal antibody (R3, Chemicon International) and subsequently reacted with 1:5000-diluted peroxidase-conjugated goat anti-mouse IgG. The membrane was treated with the ECL kit-WB detection system (Amersham) and exposed to X-ray film. Monolayer-cultured AGS-neo cells were treated with 1 μg ml^{-1} 12-*O*-tetradecanoylphorbol-13-acetate (TPA; Sigma) in six-well plates and cultured. After incubation for 2 days, cells were collected and Western blotting was carried out to detect EBV EA-D. Similarly, EBV EA-D was detected after stimulation of AGS-neo cells by *in vitro*-synthesized NH_2Cl. NH_2Cl was added at concentrations of 2, 20, 200 and 2000 μM to AGS-neo monolayers in six-well plates. After incubation for 5 min, the cells were collected, and Western blotting was carried out. Alternatively, NH_2Cl was added to AGS-neo monolayers in six-well plates at a concentration of 100 μM. After incubation for 2·5, 5, 7·5, 10, 15, 20, 30, 40, 50, 60 or 70 min, the cells were collected and Western blotting was performed. The cells were cultured for 48 h at 37 °C under the conditions described above. Then, 100 μM NH_2Cl or 100 μM NH_2Cl combined with 20 mM methionine (Sigma), which is an NH_2Cl scavenger, was added prior to immunofluorescent staining for EA-D.

Immunofluorescent staining for EA-D was carried out by indirect immunofluorescence with 1:40-diluted mouse anti-EBV EA-D-p52/50 monoclonal antibody, as described above, followed by FITC-conjugated anti-mouse IgG (Cappel) as the secondary antibody.

Flow cytometry. The expression of EBV-associated antigen, EBNA1, by AGS-neo cells, and of EA-D by Raji and B95-8 cells, was also measured by indirect immunofluorescent flow cytometric analysis using a FACSCalibur (BD Immunocytometry Systems) flow cytometer and CellQuest software. Prior to reaction with the primary antibody, cells were treated with permeabilization reagent using IntraPrep Reagent (Immunotech) according to the manufacturer's procedures, and then 1×10^5 cells were incubated on ice for 1 h with 1:40-diluted anti-EBNA1 rat monoclonal antibody (2B4-1; Dako) and anti-EBV EA-D-p52/50 mouse monoclonal antibody. FITC-conjugated anti-mouse (1:50) monoclonal antibody was used as the secondary antibody.

Gastric biopsy specimens. Seventy-eight gastric biopsy specimens were obtained from 78 patients who presented with gastrointestinal symptoms and were encouraged to undergo stomach biopsy at Oita University Hospital. All patients were examined regarding *H. pylori* infection status, which was determined by bacterial culture, histology, and urea breath test. Forty-eight patients were positive for *H. pylori* infection and the remaining 30 patients were negative. The specimens were fixed in formalin, embedded in paraffin wax, and used for *in situ* hybridization (ISH) and immunostaining. Informed consent was obtained from all patients before study participation. The study protocol was approved by the Ethics Committee of the Faculty of Medicine, Oita University.

Immunohistochemistry for EBNA1, LMP-1 and *H. pylori*, and ISH for EBER-1. Anti-EBNA1 rat monoclonal, anti-LMP-1 mouse monoclonal (S-12, Dako) and anti-*H. pylori* rabbit polyclonal (B0471, Dako) antibodies were used for the identification of the latent infection state of EBV and the localization of *H. pylori*. A standard immunoperoxidase staining procedure (Vectastain ABC kit, Vector Laboratories) was used for the antigen detection. EBER-1 was detected with a digoxigenin-labelled 30-base oligomer probe (Research Genetics), using procedures described elsewhere (Yanai *et al.*, 1997). Paraffin-embedded sections (5 μm thick) of biopsy specimens were deparaffinized, rehydrated, pre-digested with Pronase and pre-hybridized, and then hybridized overnight at 37 °C. After washing with 0·5× SSC, hybridization was detected using an anti-digoxigenin antibody alkaline phosphatase conjugate (Boehringer Mannheim) according to the manufacturer's instructions. Confluent cultured AGS-neo cells in a chamber slide (Lab-Tek, Nalge Nunc) were fixed with cold acetone and subjected to a similar ISH technique for the detection of EBER-1.

RESULTS

Characterization of EBV infection status of AGS-neo cells in the resting state and after TPA treatment

The ISH assay demonstrated that EBER-1 was abundantly transcribed in all AGS-neo cells without any lytic stimuli (Fig. 1A). Flow cytometry analysis revealed that AGS-neo cells showed apparent expression of EBNA1 in the resting state (Fig. 1B). The phorbol ester TPA is the most reproducible and widely used inducer of lytic EBV infection. The expression of EA-D antigen in AGS-neo cells was detected in the presence of TPA at a final concentration of 1 μg ml^{-1}. After the treatment with TPA, AGS-neo cells that appeared to be detached from the culture flask (lane 2, Fig. 1C) showed stronger EA-D expression than adherent cells (lane 1, Fig. 1C).

Expression of EBV EA-D after NH_2Cl treatment *in vitro*

Firstly, we determined whether or not *in vitro* synthesized NH_2Cl could induce lytic infection in B-cell lines, namely B 95-8 and Raji cells, latently infected with EBV. As shown in Fig. 2(A, B), apparent deviations of EA-D expression in B 95-8 and Raji cells were observed in the presence of 100 μM NH_2Cl. Although minimal increases were observed after 1 h of NH_2Cl treatment, the degree of increase was clearer after 48 h of treatment.

In order to investigate the induction of EBV lytic infection by NH_2Cl produced by *H. pylori* infection in gastric mucosa, we studied the effect of *in vitro* NH_2Cl on AGS-neo cells. Increased expression of EA-D was observed in a dose-dependent manner after the addition of *in vitro*-synthesized NH_2Cl (Fig. 2C). Such expression was detected as early as 2·5 min after the addition of NH_2Cl, and was sustained for almost 60 min (Fig. 2D). More than 2 h treatment of AGS-neo cells with 100 μM NH_2Cl caused a higher proportion of damaged cells, cell detachment and cell death.

Although confluent AGS-neo cells show an adherent and polygonal appearance (Fig. 3A), cell detachment (Fig. 3B) and EBV EA-D-positive cells (Fig. 3C) were observed following the addition of NH_2Cl at 100 μM. The addition of methionine (20 mM), a well-known specific scavenger of NH_2Cl, prior to the treatment with NH_2Cl completely inhibited the detachment of cells from the bottom of the culture dish (Fig. 3D). Furthermore, the addition of methionine to NH_2Cl-treated AGS-neo cells resulted in inhibition of not only the cell damage but also EA-D antigen expression (data not shown).

Immunohistochemistry of EBNA1, LMP-1 and *H. pylori* antigen expression and ISH for EBER-1 in gastric biopsy specimens

Next we explored whether EBV-infected gastric epithelium could interact with *H. pylori*, and also examined the

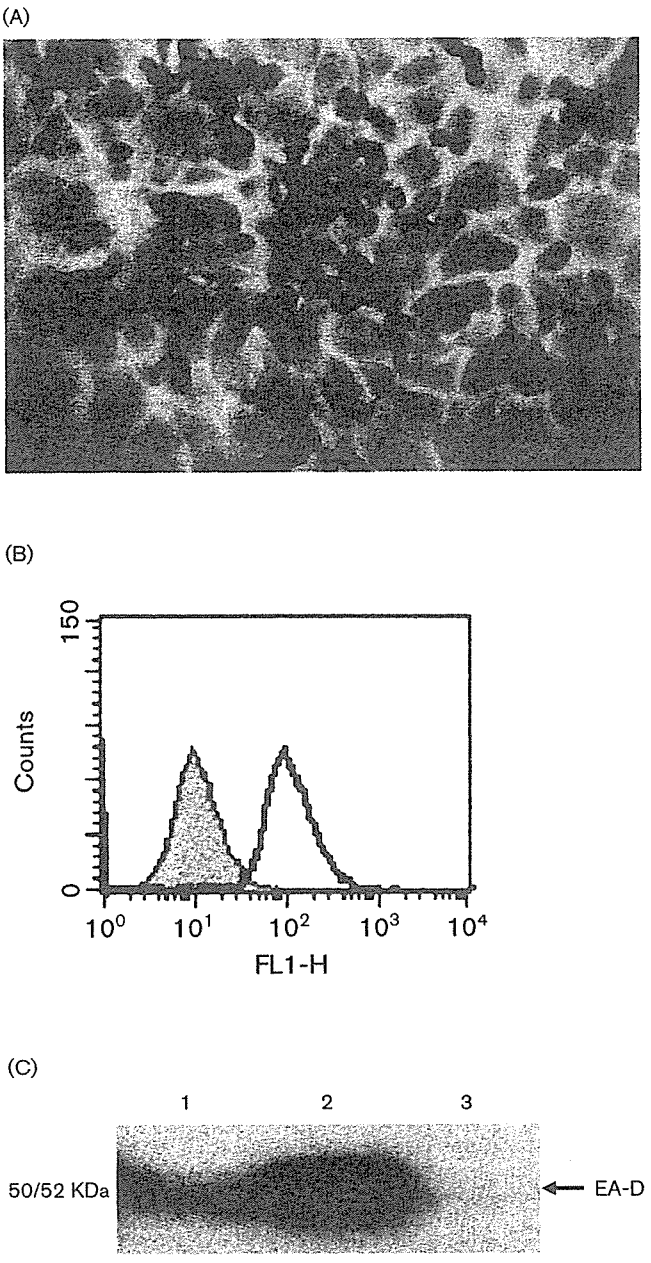

Fig. 1. Characteristics of AGS-neo cells with respect to EBV latent infection and lytic conversion induced by TPA: *in situ* detection of EBER-1 expression in AGS-neo cells. Strongly positive reactions of EBER-1 were seen in AGS-neo cells by ISH (A) and the expression of EBNA1 antigen (white peak) was examined by FACS analysis (B). The grey peak shows the expression of EBNA1 signal without primary antibody. Monolayer-cultured AGS-neo cells were treated with 1 μg TPA ml^{-1} in six-well plates, and cells were then collected separately after 2 days incubation. (C) Western blotting was carried out for the detection of EBV EA-D. Lane 1, cell lysate obtained from adherent AGS-neo cells treated with 1 mg TPA ml^{-1}; lane 2, lysate from detached AGS-neo cells treated with the same concentration of TPA; lane 3, lysate from AGS-neo cells without treatment with TPA.

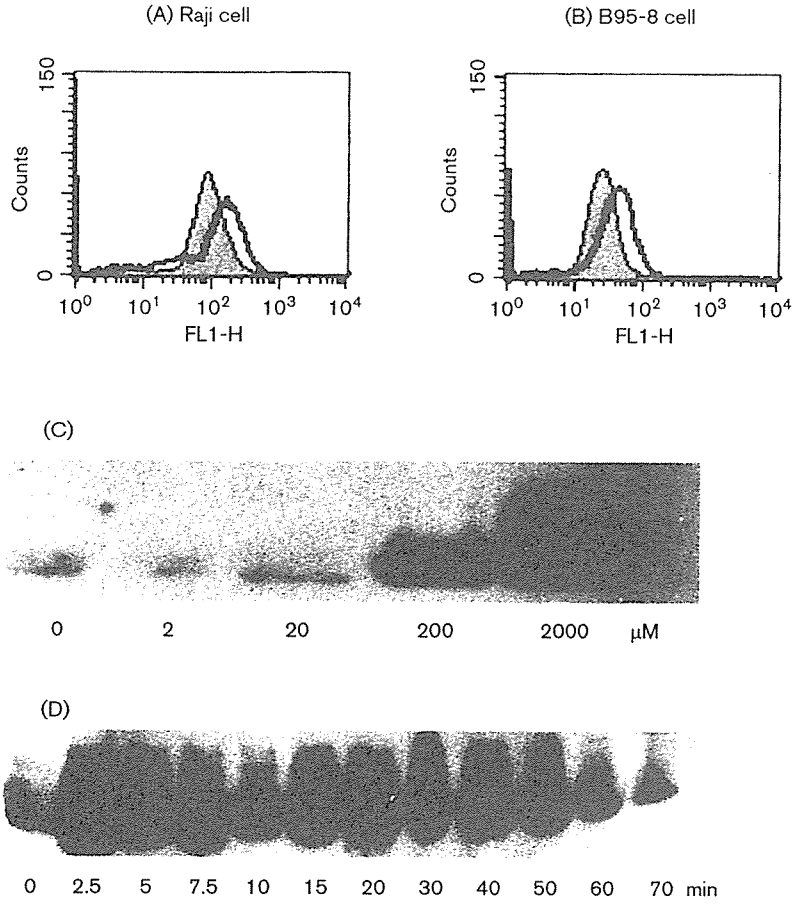

Fig. 2. Effect of NH_2Cl on EBV cells and AGS-neo cells. (A, B) Expression of EA-D antigen on the surface of Raji (A) and B95-8 (B) cells treated with NH_2Cl: after 48 h, the bold line (white peak) shows the level of EA-D antigen in cells treated at a concentration of 100 μM NH_2Cl and the thin line shows the level without NH_2Cl treatment (grey peak). (C) NH_2Cl was added at concentrations of 0, 2, 20, 200 and 2000 μM to AGS-neo monolayers placed in six-well plates. After incubation for 5 min, the cells were collected, and Western blotting was performed with anti-EBV EA-D p52/50 antibody (×5000) as the primary antibody. (D) NH_2Cl was added at a concentration of 100 μM to AGS-neo monolayers in six-well plates. After incubation for 0, 2·5, 5, 7·5, 10, 15, 20, 30, 40, 50, 60 and 70 min, the cells were collected, and Western blotting was performed. EBV EA-D was detected within 2·5 min of stimulation with NH_2Cl.

associated inflammatory changes in human specimens. Of 48 *H. pylori*-positive patients, 24 were positive for EBER-1, as determined by ISH (Table 1). In comparison, only two of 30 *H. pylori*-negative patients were positive for EBER-1 (Table 1). As shown in Fig. 4(A), the EBER-1 signal was localized in a relatively deep area of gastric mucosal layer, and goblet cell metaplasia was occasionally observed close to EBER-1-positive cells. Immunohistochemical analyses using anti-EBNA1 and anti-LMP-1 monoclonal antibodies revealed that among 48 *H. pylori*-positive patients, 18 and 13 cases were positive for EBNA1 and LMP-1 antigen, respectively (Table 1 and Fig. 4B, C). Positive expression of latent antigen was also localized in relatively deeper areas of the gastric glands. Live *H. pylori* cells densely colonized the mucosal surface of the *H. pylori*-infected gastric tissue, but not the deeper area. Inflammatory reactions characterized by dense infiltration of neutrophils and lymphocytes were recognized in the interstitial area of the gastric mucosa (Fig. 4C).

DISCUSSION

Infection with EBV occurs in most individuals. EBV is associated with several forms of human neoplasm (Rickinson & Kieff, 2001) and is also known to be an important aetiologic agent of gastric carcinoma (Shibata & Weiss, 1992). EBV infection may cause gastric carcinoma in areas of damaged gastric tissue, which is also a well-known pathological consequence of *H. pylori* infection. Previous studies of mutual interactions between *H. pylori* and EBV in the human stomach show that the clinicopathological relationship in gastric carcinogenesis remains unclear (Wu *et al.*, 2000; Shinohara *et al.*, 1998). In the present study, we speculated that these two ubiquitous pathogens, *H. pylori* and EBV, have direct or indirect relevance to environmental changes in the infected host. We assumed that *H. pylori* or its products could affect the EBV life cycle, especially the viral reactivation process.

To date, the pathogenicity of *H. pylori* has been demonstrated in terms of epithelial damage, and in particular in terms of the association with gastric carcinogenesis. We demonstrated that half of the gastric biopsy specimens from *H. pylori*-infected individuals showed positive signals for EBER-1 (Table 1), and such cryptic EBV infection might be affected by *H. pylori* infection. Firstly, we hypothesized that intracellular signal modification by cagA injection into the AGS-neo cells via type IV secretion machinery might be responsible for the EBV reactivation process (Asahi *et al.*, 2000; Higashi *et al.*, 2002; Mimuro *et al.*, 2002). However, the induction of EA-D antigen was observed at equal levels for *H. pylori* strains that possessed cagPAI and those that did

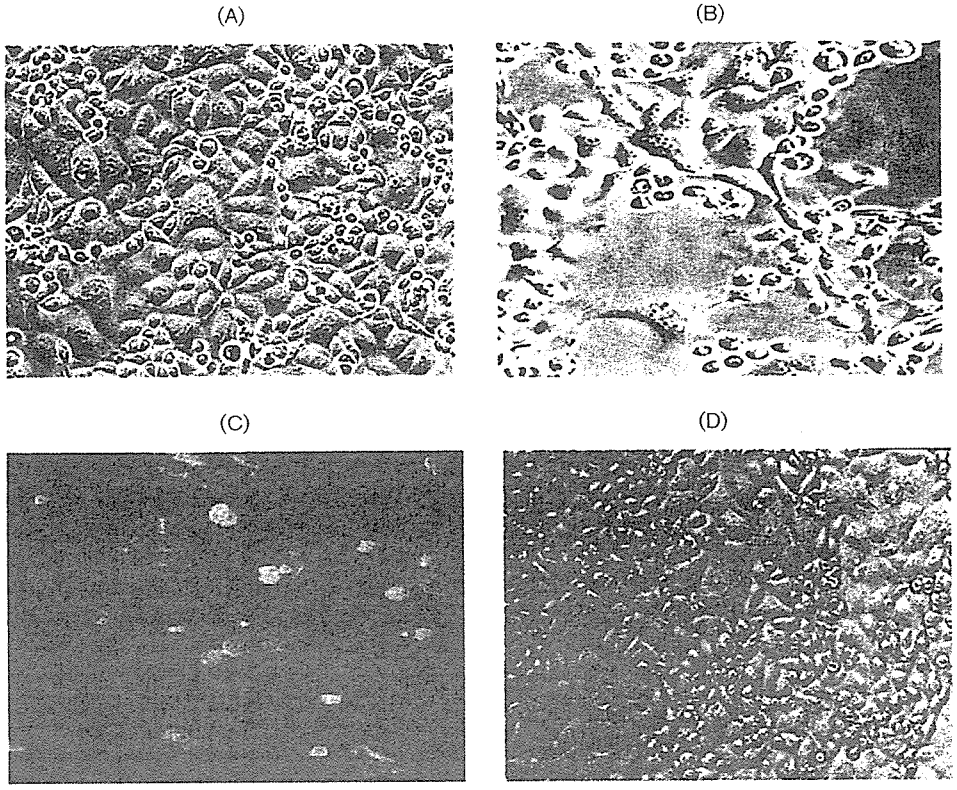

Fig. 3. NH_2Cl induces morphological changes and EA-D expression in AGS-neo cells. Microscopic findings of the effect of NH_2Cl on AGS-neo cells are shown. The cells were cultured for 48 h at 37 °C in F-12 (HAM) Nutrient Mixture medium supplemented with 10% (v/v) non-heat-inactivated FBS, 100 U penicillin ml^{-1}, 100 μg streptomycin ml^{-1} and 500 μg geneticin ml^{-1} (A). (B) NH_2Cl at 100 μM was added to the confluent AGS-neo cells and the cells were incubated for 60 min. Most cells were round, shrunken and detached from the bottom of the flask. Such damaged cells showed expression of EA-D antigen (C). When 20 mM methionine was added prior to treatment with 100 μM NH_2Cl, the cells completely retained adhesion to the culture dishes (D).

not (data not shown). Therefore, other mechanisms may be involved in EBV reactivation in the AGS-neo cells. The neutrophil-derived membrane-permeating oxidant NH_2Cl is known to induce detachment of cultured cells, concomitant with DNA damage (Suzuki *et al.*, 1997, 1998), as well as morphological changes characteristic of those caused by dephosphorylation of p-Tyr and an increase in intracellular Ca^{2+} concentration (Nakamura *et al.*, 1995). Mobilization of intracellular Ca^{2+} is closely correlated with the induction of ZEBRA protein, which is known to be the immediate early gene product encoded by BZLF1.

Table 1. Incidence of EBV gene (EBER-1) and associated antigens (EBNA1 and LMP-1) by ISH and immunostaining in *H. pylori*-infected and -uninfected individuals

+, *H. pylori* infected; −, uninfected.

Patient group	Incidence		
	EBER-1	EBNA1	LMP-1
H. pylori (+)*	24/48	18/48	13/48
H. pylori (−)	2/30	0/30	0/30

*Significantly higher frequency of EBER-1, EBNA1 and LMP-1 in the *H. pylori* (+) group in comparison with the *H. pylori* (−) group at a significance level of $P < 0{\cdot}01$ by the chi square test.

Reactivation of the EBV lytic programme in the epithelium, unlike in B lymphocytes, is not clearly understood (Faulkner *et al.*, 2000). EBV BZLF1 protein is known to inhibit host-cell proliferation by causing cell-cycle arrest in G0/G1 in several epithelial tumour cell lines (Cayrol & Flemington, 1996; Rodriguez *et al.*, 2001). After activation of the lytic programme by BZLF1 induction, B95-8 cells are arrested mainly around the G1/S boundary, and the progression from G1 to S phase, in which cellular DNA synthesis is inhibited, appears to favour viral lytic replication (Kudoh *et al.*, 2003). Therefore, the virus replication/reactivation from the latent stage and the host intracellular environment are closely related. It may be considered that EBV makes rapid and strong attempts to survive or to preserve its genome information when the infected host cells

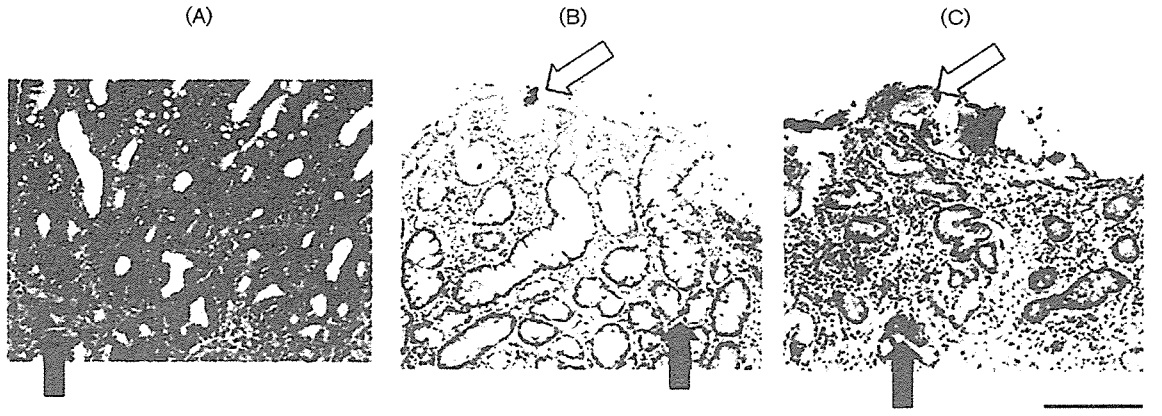

Fig. 4. Detection of EBV latent infection-associated antigens and *H. pylori* in gastric specimens colonized with *H. pylori*. (A) EBER-1 signals (closed arrow) were noted in a deep region of gastric glands with heavy goblet cell metaplasia. (B, C) *H. pylori* bacteria (open arrow) were observed on the surface of gastric epithelium. EBV latent antigen EBNA1 (B, closed arrow) and LMP-1 (C, closed arrow) showed positive reactions in the middle or lower layer of the gastric glandular region with inflammation. Bar, 0·4 mm.

are confronted with a crisis or death situation (Hoshikawa *et al.*, 2002).

Our study indicates for the first time that the *H. pylori*-associated oxidant NH_2Cl is able to induce the lytic conversion of latent EBV infection. Moreover, the switching of EBV from the latent to the lytic phase occurred very rapidly, which should enable the virus to survive or maintain the viral genome, because exposure to higher concentrations (>100 μM) of NH_2Cl for over 2 h resulted in cell death (Nakamura *et al.*, 1995), mediated by a 'peeling off' phenomenon characterized by marked morphological changes with cell detachment, ballooning and hypercontraction. We speculate that the expression of EA-D antigen in AGS-neo cells is closely associated with the morphological changes that occur during the EBV reactivation process. In a preliminary study, we found by fluorescence-activated cell sorting (FACS) analysis that the expression of Annexin V of AGS-neo cells increased immediately after treatment (within 2·5 min) with 100 μM NH_2Cl, and whereas the proportion of viable cells in the presence of 100 μM NH_2Cl was more than 90 % up to 2·5 min, the proportion decreased by more than 50 % after 60 min in the presence of the same concentration of NH_2Cl (data not shown). Following the reactivation of the expression of EBV early gene products by *H. pylori* infection or NH_2Cl treatment, progeny virus will be released from the AGS-neo cells. Supernatants from *H. pylori*-infected AGS-neo cells successfully transformed peripheral B lymphocytes and showed EBNA1 expression in their cytoplasm (data not shown). These observations are consistent with the hypothesis that EBV reactivation and newly synthesized viral production occur during *H. pylori* infection in the human stomach.

In conclusion, *H. pylori*-associated gastric inflammation induces the production of the oxidant NH_2Cl, derived from infiltrating neutrophils, and this converts the latent EBV infection to infection with activation of the early gene, resulting in the induction of lytic EBV infection.

ACKNOWLEDGEMENTS

The authors gratefully acknowledge Professor Kenzo Takada and Dr Hironori Yoshiyama, Department of Virology, Cancer Institute, Hokkaido University School of Medicine, for providing AGS-neo cells. We thank Professor Takeshi Sairenji, Department of Biosignalling, School of Life Science, Faculty of Medicine, Tottori University, for helpful discussions and also thank Mr Shinji Yano and Kiyomi Ohno for excellent technical assistance.

REFERENCES

Asahi, M., Azuma, T., Ito, S. & 9 other authors (2000). *Helicobacter pylori* CagA protein can be tyrosine phosphorylated in gastric epithelial cells. *J Exp Med* **191**, 593–602.

Cayrol, C. & Flemington, E. (1996). G0/G1 growth arrest mediated by a region encompassing the basic leucine zipper (bZIP) domain of the Epstein–Barr virus transactivator Zta. *J Biol Chem* **271**, 31799–31802.

Faulkner, G. C., Krajewski, A. S. & Crawford, D. H. (2000). The ins and outs of EBV infection. *Trends Microbiol* **8**, 185–189.

Fukayama, M., Hayashi, Y., Iwasaki, Y. & 7 other authors (1994). Epstein–Barr virus-associated gastric carcinoma and Epstein–Barr virus infection of the stomach. *Lab Invest* **71**, 73–81.

Gradoville, L., Kwa, D., El-Guindy, A. & Miller, G. (2002). Protein kinase C-independent activation of the Epstein–Barr virus lytic cycle. *J Virol* **76**, 5612–5626.

Grisham, M. B., Gaginella, T. S., von Ritter, C., Tamai, H., Be, R. M. & Granger, D. N. (1990). Effects of neutrophil-derived oxidants on intestinal permeability, electrolyte transport, and epithelial cell viability. *Inflammation* **14**, 531–542.

Higashi, H., Tsutsumi, R., Muto, S., Sugiyama, T., Azuma, T., Asaka, M. & Hatakeyama, M. (2002). SHP-2 tyrosine phosphatase as

an intracellular target of *Helicobacter pylori* CagA protein. *Science* **295**, 683–686.

Hoshikawa, Y., Satoh, Y., Murakami, M., Maeta, M., Kaibara, N., Ito, H., Kurata, T. & Sairenji, T. (2002). Evidence of lytic infection of Epstein–Barr virus (EBV) in EBV-positive gastric carcinoma. *J Med Virol* **66**, 351–359.

Imai, S., Koizumi, S., Sugiura, M., Tokunaga, M., Uemura, Y., Yamamoto, N., Tanaka, S., Sato, E. & Osato, T. (1994). Gastric carcinoma: monoclonal epithelial malignant cells expressing Epstein–Barr virus latent infection protein. *Proc Natl Acad Sci U S A* **91**, 9131–9135.

Janz, A., Oezel, M., Kurzeder, C., Mautner, J., Pich, D., Kost, M., Hammerschmidt, W. & Delecluse, H. J. (2000). Infectious Epstein–Barr virus lacking major glycoprotein BLLF1 (gp350/220) demonstrates the existence of additional viral ligands. *J Virol* **74**, 10142–10152.

Kieff, E. & Rickinson, A. B. (2001). Epstein–Barr virus. In *Fields Virology*, pp. 2511–2573. Edited by D. M. Knipe & P. M. Howley. Philadelphia: Lippincott Williams & Wilkins.

Kudoh, A., Fujita, M., Kiyono, T., Kuzushima, K., Sugaya, Y., Izuta, S., Nishiyama, Y. & Tsurumi, T. (2003). Reactivation of lytic replication from B cells latently infected with Epstein–Barr virus occurs with high S-phase cyclin-dependent kinase activity while inhibiting cellular DNA replication. *J Virol* **77**, 851–861.

Mimuro, H., Suzuki, T., Tanaka, J., Asahi, M., Haas, R. & Sasakawa, C. (2002). Grb2 is a key mediator of *Helicobacter pylori* CagA protein activities. *Mol Cell* **10**, 745–755.

Morris, A. & Nicholson, G. (1987). Ingestion of *Campylobacter pyloridis* causes gastritis and raised fasting gastric pH. *Am J Gastroenterol* **82**, 192–199.

Murakami, M., Asagoe, K., Dekigai, H., Kusaka, S., Saita, H. & Kita, T. (1995). Products of neutrophil metabolism increase ammonia-induced gastric mucosal damage. *Dig Dis Sci* **40**, 268–273.

Nakamura, T. Y., Yamamoto, I., Nishitani, H., Matozaki, T., Suzuki, T., Wakabayashi, S., Shigekawa, M. & Goshima, K. (1995). Detachment of cultured cells from the substratum induced by the neutrophil-derived oxidant NH_2Cl: synergistic role of phosphotyrosine and intracellular Ca^{2+} concentration. *J Cell Biol* **131**, 509–524.

Nomura, A., Stemmermann, G. N., Chyou, P. H., Kato, I., Perez-Perez, G. I. & Blaser, M. J. (1991). *Helicobacter pylori* infection and gastric carcinoma among Japanese Americans in Hawaii. *N Engl J Med* **325**, 1132–1136.

Parsonnet, J., Friedman, G. D., Vandersteen, D. P., Chang, Y., Vogelman, J. H., Orentreich, N. & Sibley, R. K. (1991). *Helicobacter pylori* infection and the risk of gastric carcinoma. *N Engl J Med* **325**, 1127–1131.

Rickinson, A. B. & Kieff, E. (2001). Epstein–Barr virus. In *Fields Virology*, pp. 2575–2627. Edited by D. M. Knipe & P. M. Howley. Philadelphia: Lippincott Williams & Wilkins.

Rodriguez, A., Jung, E. J., Yin, Q., Cayrol, C. & Flemington, E. K. (2001). Role of c-myc regulation in Zta-mediated induction of the cyclin-dependent kinase inhibitors p21 and p27 and cell growth arrest. *Virology* **284**, 159–169.

Sato, K., Watanabe, S., Yoshizawa, T., Hirose, M., Murai, T. & Sato, N. (1999). Ammonia, hydrogen peroxide, and monochloramine retard gastric epithelial restoration in rabbit cultured cell model. *Dig Dis Sci* **44**, 2429–2434.

Shibata, D. & Weiss, L. M. (1992). Epstein–Barr virus-associated gastric adenocarcinoma. *Am J Pathol* **140**, 769–774.

Shinohara, K., Miyazaki, K., Noda, N., Saitoh, D., Terada, M. & Wakasugi, H. (1998). Gastric diseases related to *Helicobacter pylori* and Epstein–Barr virus infection. *Microbiol Immunol* **42**, 415–421.

Sumie, A., Yamashiro, T., Nakashima, K., Nasu, M., Watanabe, M. & Nishizono, A. (2001). Comparison of genomic structures and antigenic reactivities of orthologous 29-kilodalton outer membrane proteins of *Helicobacter pylori*. *Infect Immun* **69**, 6846–6852.

Suzuki, M., Miura, S., Suematsu, M. & 7 other authors (1992). *Helicobacter pylori*-associated ammonia production enhances neutrophil-dependent gastric mucosal cell injury. *Am J Physiol* **263**, G719–G725.

Suzuki, H., Mori, M., Suzuki, M., Sakurai, K., Miura, S. & Ishii, H. (1997). Extensive DNA damage induced by monochloramine in gastric cells. *Cancer Lett* **115**, 243–248.

Suzuki, H., Seto, K., Mori, M., Suzuki, M., Miura, S. & Ishii, H. (1998). Monochloramine induced DNA fragmentation in gastric cell line MKN45. *Am J Physiol* **275**, G712–G716.

Wu, M. S., Shun, C. T., Wu, C. C., Hsu, T. Y., Lin, M. T., Chang, M. C., Wang, H. P. & Lin, J. T. (2000). Epstein–Barr virus-associated gastric carcinomas: relation to *H. pylori* infection and genetic alterations. *Gastroenterology* **118**, 1031–1038.

Yanai, H., Takada, K., Shimizu, N., Mizugaki, Y., Tada, M. & Okita, K. (1997). Epstein–Barr virus infection in non-carcinomatous gastric epithelium. *J Pathol* **183**, 293–298.

Yoshiyama, H., Imai, S., Shimizu, N. & Takada, K. (1997). Epstein–Barr virus infection of human gastric carcinoma cells: implication of the existence of a new virus receptor different from CD21. *J Virol* **71**, 5688–5691.

INFECTION AND IMMUNITY, Feb. 2006, p. 984–993 Vol. 74, No. 2
0019-9567/06/$08.00+0 doi:10.1128/IAI.74.2.984–993.2006

Transfer of Antigen-Pulsed Dendritic Cells Induces Specific T-Cell Proliferation and a Therapeutic Effect against Long-Term *Helicobacter pylori* Infection in Mice

Satoshi Otsu,[1] Kazuyo Gotoh,[1] Tetsu Yamashiro,[2] Junpei Yamagata,[1] Kouichirou Shin,[3] Toshio Fujioka,[4] and Akira Nishizono[1]*

Department of Infectious Diseases (Microbiology[1] and General Medicine[4]) and Institute of Scientific Research,[2] Faculty of Medicine, Oita University, Oita, and Nutritional Science Laboratory, Morinaga Milk Industry Co. Ltd., Kanagawa,[3] Japan

Received 20 July 2005/Returned for modification 23 August 2005/Accepted 26 October 2005

***Helicobacter pylori* causes persistent infection of the stomach and results in chronic gastritis and peptic ulcers. Jaws II cells, derived from mouse bone marrow, were pulsed with live or formalin-killed or whole-cell sonicates (WCS) of *H. pylori*. Representative cell surface molecules were expressed at substantial levels on Jaws II cells, indicating that appropriate maturation of the cells was achieved with the three *H. pylori* antigens without any significant differences. *H. pylori* WCS-pulsed Jaws II cells secreted a significant amount of tumor necrosis factor alpha into the culture supernatant. The naïve T cells exposed to the WCS-pulsed Jaws II cells showed significant proliferation and gamma interferon (IFN-γ) and interleukin-10 (IL-10) production in vitro. A 2-log reduction in the number of colonizing bacteria was observed in the mice treated with the WCS-pulsed Jaws II cells; however, no significant reductions were achieved in mice treated with Jaws II cells pulsed with other *H. pylori* antigens. Up-regulated production of IFN-γ and IL-10 was observed in the stomachs of the mice treated with the WCS-pulsed Jaws II cells, which is consistent with the result obtained in vitro. There were no differences in gastritis scores or *H. pylori*-specific antibody titers among the mice treated with Jaws II cells pulsed with the three different *H. pylori* antigens. The results suggest that Th1 cell-mediated immunity in combination with Th2 cell-mediated immunity plays a role in reducing colonizing bacterial numbers in mice with chronic *H. pylori* infections.**

Helicobacter pylori is a gram-negative curved bacterium that colonizes the human stomach and causes chronic gastric diseases. It is recognized as the etiologic agent of atrophic gastritis, peptic ulcers, intestinal metaplasia, mucosa-associated lymphoid tissue lymphoma, and gastric cancer.

Transmission of and infection with *H. pylori* occur mainly through female carriers via heavy contact or upon food and/or water intake during childhood before approximately 5 years of age. When an infection is established, *H. pylori* antigen-specific antibodies are developed and their production is sustained throughout the entire period of infection. Such a specific response, however, does not seem to be associated with a reduction in the number of *H. pylori* bacteria colonizing the stomach (6, 11, 37). With regard to reducing the number of colonizing *H. pylori* bacteria, cellular immunity has been reported to play the principal role where Th1-polarized rather than Th2-polarized T cells recruit mononuclear cells to the site of infection (34), resulting in elimination of the bacteria (4, 18). Meanwhile, *H. pylori* has evolved to evade not only the innate but also the adaptive immune response. For example, the antigen-dependent proliferation of T cells is specifically blocked by *H. pylori*: an intracellular T-cell mechanism is directly disrupted by secreted and internalized VacA protein. An antigenic alteration via a frameshift (28, 38) or a nucleotide transfer (36) was reported likely to occur in an outer membrane protein which facilitates bacterial evasion of the host immune system. All this allows *H. pylori* to evade the host immune system, leading to a persistent infection in the stomach.

Triple therapy, typically consisting of two antibiotics plus a proton pump inhibitor, has become "the gold standard" for treatment to eradicate *H. pylori*; however, adverse reactions including allergies, hepatic disorders, and diarrhea remain to be overcome. Add to this the emergence of antibiotic-resistant bacteria and the situation becomes complicated.

Dendritic cells (DCs) have important functions such as antigen presentation and cytokine secretion in the innate as well as the adaptive immune system (35). They drive the host immune reaction by modulating the functions or interactions of effector cells like $CD4^+$ and $CD8^+$ cells, macrophages, and B cells. The immunomodulatory function of DCs has prompted researchers to work on utilizing these cells for controlling neoplasmic diseases and allergic disorders (1, 26, 30). The treatment of infectious diseases is another area where DC-related immunomodulation therapy could be effective. Several DC-related works focusing on acute *Listeria monocytogenes* (32) infection and *Streptococcus pneumoniae* (3) infection have been launched; however, the number of works regarding chronic persistent infection is limited (5, 7).

In an attempt to provide an option other than triple therapy, we have studied the effectiveness of preventive or therapeutic vaccinations against *H. pylori* infection (13, 16, 22, 23), the mechanisms of which remain to be clarified. In the present study, we examined whether DCs pulsed with *H. pylori* antigens

* Corresponding author. Mailing address: Department of Infectious Diseases (Microbiology), Faculty of Medicine, Oita University, Idaigaoka 1-1, Hasama-machi, Oita 879-5593, Japan. Phone: 81-97-586-5710. Fax: 81-97-586-5719. E-mail: a24zono@med.oita-u.ac.jp.

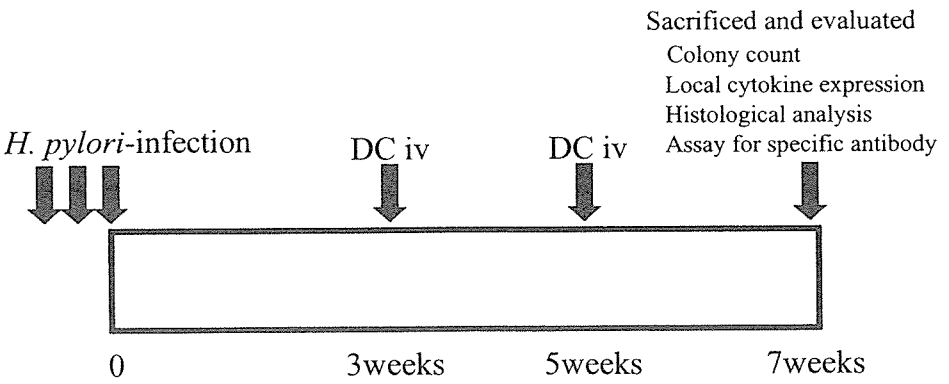

FIG. 1. Protocols for *H. pylori* infection and administration of antigen-pulsed or unpulsed Jaws II cells used in this study. Mice were infected orally with the *H. pylori* inoculum (0.5×10^8 CFU) three times and divided into five groups. The mice in each group were intravenously treated with 1.25×10^5 (100 μl) *H. pylori* antigen (LB, FKB, or WCS)-pulsed or unpulsed Jaws II cells at 3 and 5 weeks after the last bacterial inoculation. The densities of colonizing bacteria, severities of gastritis, and levels of *H. pylori*-specific antibodies and local cytokines were compared to those in mice treated with PBS alone.

reduced bacterial loads in the stomachs of mice with chronic *H. pylori* infections and tried to clarify the mechanisms involved to test the feasibility of DC-based immunotherapy against chronic *H. pylori* infection.

MATERIALS AND METHODS

DCs. A DC line, Jaws II, was purchased from the American Type Culture Collection. Jaws II cells were originally isolated from bone marrow cultures of C57BL/6 mice deficient in p53. The cells were grown in a complete culture medium consisting of RPMI 1640 medium with glutamax (Gibco BRL, Grand Island, NY) supplemented with 10% fetal bovine serum (Equitech-Bio, Inc., Kerrville, TX), 1% penicillin-streptomycin, 50 μM 2-mercaptoethanol, and 5 ng of recombinant mouse granulocyte-macrophage colony-stimulating factor (BD Biosciences, San Jose, CA)/ml.

Bacterial strain and *H. pylori* antigen preparations. *H. pylori* Sydney strain (SS1) stocked in our laboratory was grown in *Brucella* broth containing 10% fetal calf serum under microaerobic conditions (5%O_2, 10%CO_2, and 85% N_2) at 37°C for 24 h and used for the inoculation of mice or for the preparation of *H. pylori*-related antigens for pulsing of Jaws II cells. *H. pylori* sediment from ca. 25 ml of culture was suspended in 5 ml of normal saline solution (NSS) and used as the preparation containing live bacteria (LB). For the preparation containing formalin-killed bacteria (FKB), formalin was added at 0.5% to the LB preparation, and the mixture was left at room temperature for 24 h and vigorously washed. For the preparation containing whole-cell sonicates (WCS), the LB preparation was sonicated three times on ice and filtered with a 0.45-μm-pore-sized filter.

Flow cytometry. The expression of cell surface molecules was measured by indirect immunofluorescent flow cytometric analysis using a FACSCalibur (BD Immunocytometry Systems, San Jose, CA) flow cytometer and CellQuest software. Antigen-pulsed or unpulsed Jaws II cells (10^5) were incubated on ice for 1 h with a panel of primary antibodies, rat anti-mouse CD11b (1:50), hamster anti-mouse CD11c (1:50), rat anti-mouse CD8α (1:50), rat anti-mouse CD40 (1:50; eBioscience, San Diego, CA), mouse anti-mouse major histocompatibility complex (MHC) class I (1:50; BD Pharmingen, San Jose, CA), rat anti-mouse MHC class II (1:50; BD Biosciences), rat anti-mouse CD80 (1:50), and rat anti-mouse CD86 (1:50; provided by Hideo Yagita and Ko Okumura, Department of Immunology, University of Juntendo, Tokyo, Japan). Fluorescein isothiocyanate (FITC)-conjugated anti-rat (1:50), anti-hamster (1:50), or rat anti-mouse (1:50) monoclonal antibody was used as the secondary antibody.

Pulsing of Jaws II cells with *H. pylori*-related antigens. For the pulsing of Jaws II cells with *H. pylori*-related antigens, ca. 100 μl (WCS preparation) to 200 μl (LB and FKB preparations) of *H. pylori*-related antigens was added to 60 to 80% confluent Jaws II cells in a 6-well culture plate and incubated at 37°C for 48 h. The number of bacteria in 200 μl of the LB or FKB preparation was 20-fold the number of Jaws II cells (multiplicity of infection, 20). The fluids of each culture were collected 12, 24, and 48 h after addition of the antigen, and tumor necrosis factor alpha (TNF-α) was analyzed with an enzyme-linked immunosorbent assay (ELISA) kit (eBioscience). The *H. pylori*-related antigen-pulsed Jaws II cells were extensively washed, suspended in phosphate-buffered saline (PBS), and used for experiments with mice.

Effect of *H. pylori*-related antigen-pulsed Jaws II cells on naïve T cells. The naïve-T-cell-rich fraction was obtained from spleens of normal C57BL/6 mice by the magnetic cell sorting method (Miletenyi Biotec, Bergisch Gladbach, Germany). *H. pylori*-related antigen (LB, FKB, and WCS)-pulsed Jaws II cells were fixed with 0.75% formalin for 30 min on ice prior to exposure to the naïve T cells. The formalin-fixed Jaws II cells (1.0×10^4) were added to ca. 2×10^5 naïve T cells (1:20) cultured in a well of a 96-well flat-bottom culture plate and incubated for 72 h (8, 19). The clonal proliferation of T cells exposed to LB-, FKB-, and WCS-pulsed Jaws II cells was assayed using 5-bromo-2′-deoxyuridine (BrdU) (15) and compared to that of T cells exposed to unpulsed Jaws II cells. Briefly, 2×10^{-4} mmol of BrdU was added to each well, and the plate was incubated at 37°C for 2 h. The amount of BrdU incorporated into the T cells was measured using the anti-BrdU monoclonal antibody in the ELISA kit (Roche Switzerland).

Gamma interferon (IFN-γ) and interleukin-10 (IL-10) production was determined using the culture medium of T cells exposed to LB-, FKB-, and WCS-pulsed Jaws II cells. The culture medium was harvested at 24, 48, 72, and 96 h postexposure, and the cytokines were detected with ELISA kits (eBioscience) and compared to those in the medium of T cells exposed to unpulsed Jaws II cells.

Administration of *H. pylori*-related antigen-pulsed Jaws II cells to mice with chronic *H. pylori* infections. Specific-pathogen-free 5-week-old female C57BL/6 mice (Seac Yoshitomi, Fukuoka, Japan) that had been kept and fed appropriately were used for the experiment. Thirty-three mice were infected orally with the *H. pylori* inoculum (0.5×10^8 CFU) three times every other day and randomly divided into five groups. Each mouse was intravenously treated with 1.25×10^5 (100 μl) Jaws II cells or PBS (100 μl) alone at 3 and 5 weeks after the last bacterial inoculation. The groups treated with LB-pulsed, FKB-pulsed, and WCS-pulsed Jaws II cells were referred to as group 2 (G2; $n = 7$), group 3 (G3; $n = 7$), and group 4 (G4; $n = 7$), respectively. The densities of colonizing bacteria, severities of gastritis, and levels of *H. pylori*-specific antibodies and local cytokines in mice of each group were compared to those in mice treated with PBS alone (group 1 [G1; $n = 6$]) and mice treated with unpulsed Jaws II cells (group 5 [G5; $n = 6$]). At 2 weeks after the last administration of antigen-pulsed Jaws II cells (7 weeks after the initial inoculation), all mice were sacrificed and each stomach was excised, washed with NSS, and cut longitudinally into two pieces. One half was used for evaluating the density of colonizing *H. pylori* and local cytokine expression by quantitative real-time PCR analysis, and the other half was used for evaluating the severity of gastritis by histology (Fig. 1). All animal experiments were performed under the guidelines of the Ethics Committee for Animal Experiments of Oita University, Oita, Japan.

***H. pylori* colony count.** One half of the excised stomach was homogenized in 500 μl of NSS with a glass homogenizer (IWAKI Glass Co. Ltd., Tokyo, Japan). Fifty microliters of the gastric homogenate was serially diluted with NSS and inoculated onto M-BHM pylori agar plates (Nikken Biomedical Laboratory, Kyoto, Japan) at 37°C for 4 days under microaerobic conditions. Colonies with

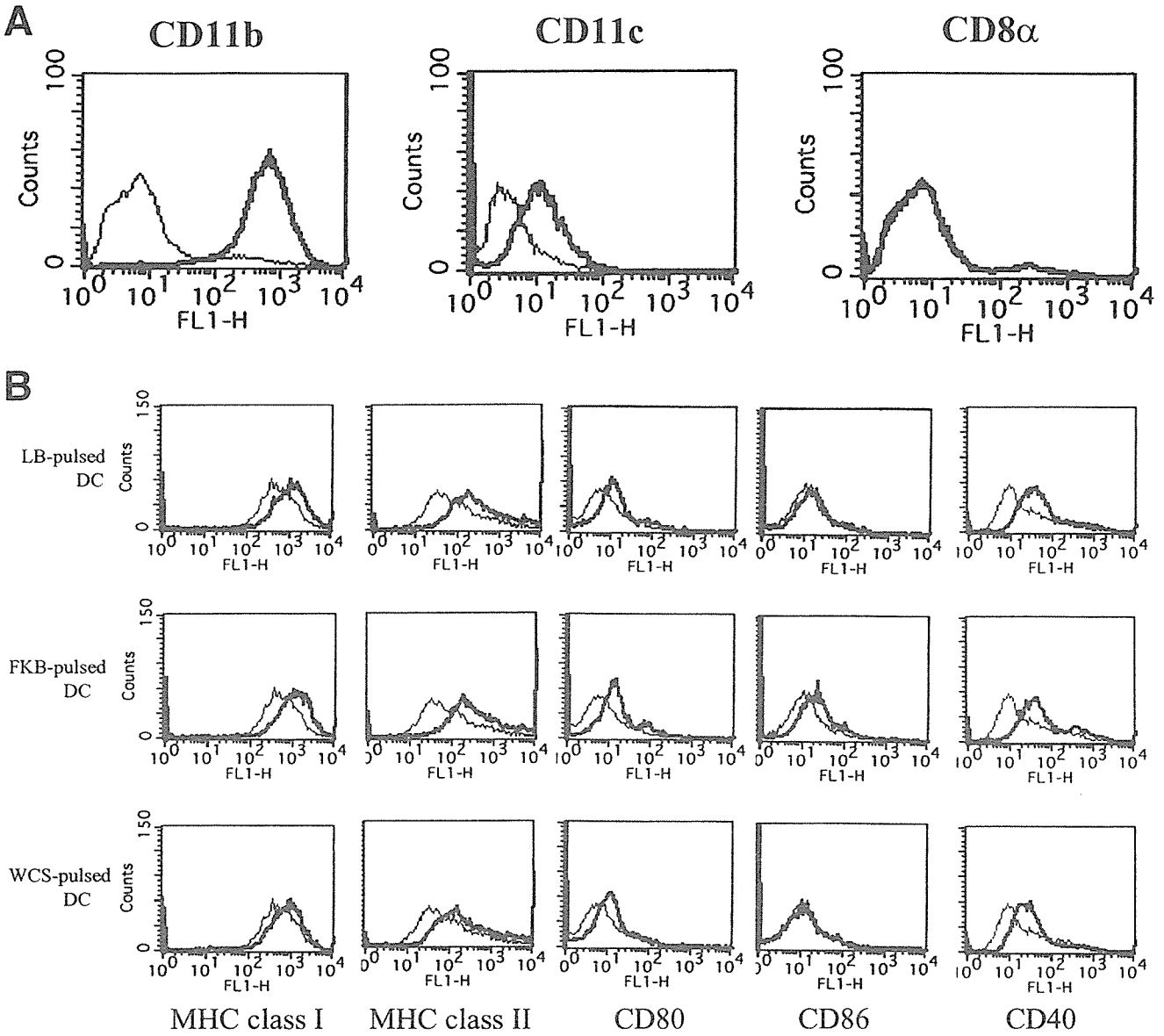

FIG. 2. Expression of cell surface molecules was measured by FACS. (A) Naïve Jaws II cells were reacted with rat anti-mouse CD11b (1:50), hamster anti-mouse CD11c (1:50), or rat anti-mouse CD8α (1:50), followed by FITC-conjugated anti-rat (1:50) or anti-hamster (1:50) monoclonal antibody. An assay was performed to confirm that the Jaws II cells used are myeloid-type DCs. (B) Jaws II cells pulsed with LB, FKB, or WCS were reacted with mouse anti-mouse MHC class I (1:50), rat anti-mouse MHC class II (1:50), rat anti-mouse CD80 (1:50), rat anti-mouse CD86 (1:50), or rat anti-mouse CD40 (1:50) and then FITC-conjugated anti-mouse (1:50) or anti-rat (1:50) monoclonal antibody. Note that appropriate maturation of the Jaws II cells was achieved with the three antigens. Obvious differences were not observed for the three antigens.

a characteristic *H. pylori* appearance were counted, and the density of the bacteria per 1.0 g of stomach tissue was calculated.

Local cytokine expression assay by quantitative real-time PCR analysis. Total RNA was extracted from the remaining 450 μl of the gastric homogenate by the acid guanidium thiocyanate-phenol chloroform method as described previously (13). Approximately 1.0 μg of the total RNA was used for a reverse transcription reaction in a 40-μl mixture containing 50 mM Tris-HCl (pH 8.3), 75 mM KCl, 3 mM $MgCl_2$, 5 mM dithiothreitol, 500 mM deoxynucleoside triphosphates, 1 mM oligo(dT) 15 primer, 20 U of RNase inhibitor (Toyobo Biomedicals, Osaka, Japan), and 500 U of Moloney murine leukemia virus reverse transcriptase (Invitrogen, Carlsbad, CA), and the mixture was incubated at 37°C for 2 h. Real-time PCR was performed using the synthesized cDNA as the template on the Smart cycler (TaKaRa, Tokyo, Japan) as described elsewhere (21). Briefly, the reaction mixture (25 μl) contained ca. 1 ng of cDNA, 1.25 U of Ex *Taq* real-time PCR version polymerase (TaKaRa), 2.5 μl of 10× real-time PCR buffer, 2.5 mM $MgCl_2$, 10 mM (each) deoxynucleotide triphosphates, SYBR green I solution at a final concentration of 5× (Cambrex Bio Science, East Rutherford, NJ), and 5 μM (each) primers as follows: β-actin, 5′-ATGGATG ACGATATCGCT-3′ (sense) and 5′-ATGAGGTAGTCTGTCTGTCAGGT-3′ (antisense); IFN-γ, 5′-CCTGCAGAGCCAGATTATCTCTTTCTACC-3′ (sense) and 5′-CCACCCCGAATCAGCAGCGA-3′ (antisense); and IL-12, 5′-TGGAAGCACGGCAGCAGAATAAAT-3′ (sense) and 5′-TGCGCTGGATT CGAACAAAGAACT-3′ (antisense). PCRs with 45 cycles of 95°C for 10 s, 55°C for 30 s, 72°C for 60 s, and 87°C for 6 s for β-actin; 45 cycles of 95°C for 10 s, 69°C for 10 s, and 87°C for 6 s for IFN-γ; and 45 cycles of 95°C for 10 s, 61°C for 45 s, and 87°C for 6 s for IL-12 were carried out. Standard curves (linear regression lines) were generated using external standards (serial 10-fold dilutions of each cytokine DNA molecule with a known copy number stocked in our laboratory)

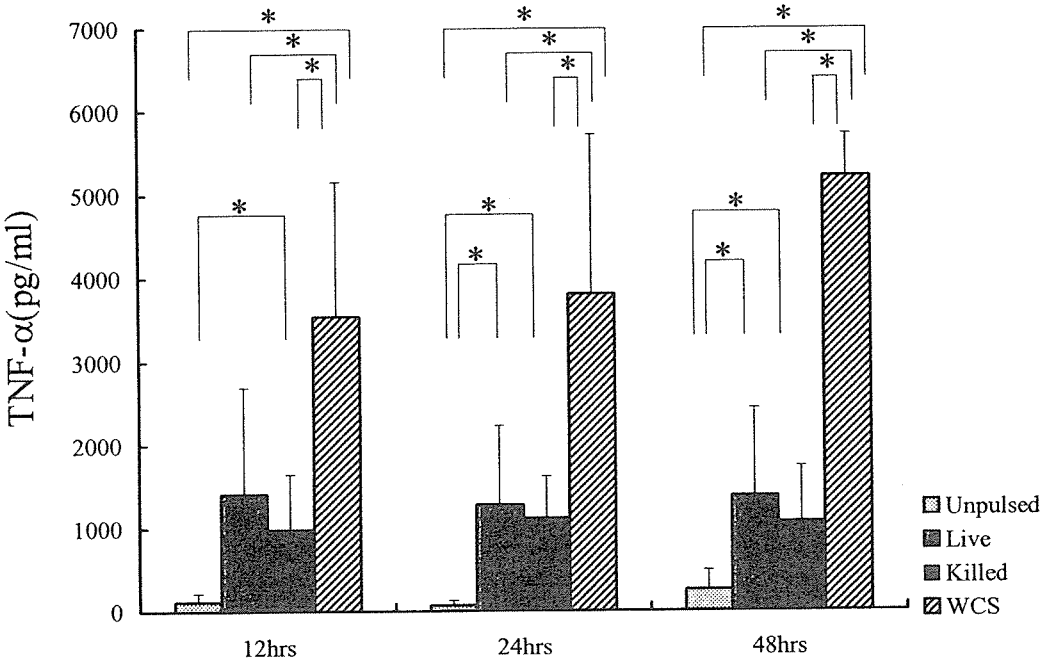

FIG. 3. TNF-α expression in Jaws II cells pulsed with LB, FKB, or WCS of *H. pylori* was analyzed. Each culture fluid was obtained at 12, 24, and 48 h after the addition of each antigen and evaluated by ELISA. Note that a significant elevation in the level of TNF-α in the supernatant of the WCS-pulsed Jaws II cells was observed at 12 h and sustained for up to 48 h postexposure. The asterisks indicate statistical significance at P of <0.05. The results are expressed as the means ± standard deviations of results for three independent cultures.

and used to estimate mRNA copy numbers in each sample. All data were standardized to results obtained for β-actin.

Histological analysis. The remaining half of each stomach was used for standard histological procedures and stained with hematoxylin and eosin for evaluation of the intensity of inflammation as described by Goto et al. (13). The severity of inflammation was scored as either 0 for no inflammation, 1 for mild inflammation, 2 for moderate inflammation, or 3 for severe inflammation. Each sample was examined two times, and the mean of the two scores was expressed as the gastritis score.

Assay for *H. pylori*-specific antibody. Blood samples were taken from mice in each group at the time of sacrifice, and whole immunoglobulin G (IgG), IgG1, IgG2a, and IgA titers were determined by ELISA. Briefly, a microtiter plate (Nunc, Roskilde, Denmark) coated with ca. 1.0 μg of *H. pylori* WCS in carbonate buffer (pH 9.6) was blocked with 5% bovine serum albumin and then each serum sample was added. Peroxidase-conjugated goat anti-mouse IgG, IgG1, IgG2a, or IgA antibody was added, and the plate was incubated at 37°C for 1 h. After several washes with PBS containing 0.05% Tween 20, the conjugated peroxidase was visualized using the tetramethylbenzidine substrate reagent set (BD Pharmingen) and absorbance was determined at an optical density of 450 nm. Each sample was tested three times.

Statistical analysis. Specific antibody titers, *H. pylori* colony counts, expression levels of cytokines, and levels of naïve-T-cell proliferation were analyzed and compared by the t test. Gastritis inflammation scores were compared using the Kruskal-Wallis test. P values of <0.05 were considered to indicate significant difference.

RESULTS

Confirmation of DC subtype and evaluation of surface molecule expression on Jaws II cells by pulsing with *H. pylori*-specific antigens. In the analysis by fluorescence-activated cell sorting (FACS), CD11b and CD11c were detected whereas CD8α was not, indicating that the Jaws II cells were myeloid-type DCs (Fig. 2A) as previously reported (17, 27, 33). When Jaws II cells were pulsed with three types of *H. pylori*-derived antigens, LB, FKB, and WCS, MHC class I antigens, MHC class II antigens, CD80, CD86, and CD40 were expressed on the cell surfaces (Fig. 2B), indicating that appropriate maturation of the Jaws II cells was achieved with those three antigens. No obvious differences in the quantities produced were observed for the three antigens used (Fig. 2B). The immature form of the DCs, with a round and nonadherent phenotype, was rendered adherent with a characteristic dendritic form as surface marker molecules were expressed (data not shown). The production of TNF-α by Jaws II cells pulsed with three different *H. pylori*-derived antigens (LB, FKB, and WCS) was analyzed by ELISA. Culture supernatants of the antigen-pulsed DCs were obtained at 12, 24, and 48 h after the addition of each antigen. A dramatic elevation in the level of TNF-α in the supernatant of the WCS-pulsed Jaws II cells was observed at 12 h. The ELISA-determined TNF-α titer for the WCS-pulsed Jaws II cells was significantly higher, exceeding 3,500 pg/ml, than those for the unpulsed Jaws II cells or the LB- or FKB-pulsed Jaws II cells. The higher TNF-α titer detected in the supernatant of WCS-pulsed Jaws II cells was sustained for up to 48 h, whereas no obvious increase was observed in the culture medium obtained from the LB- or the FKB-pulsed Jaws II cells (Fig. 3). Elevated levels of IL-10 or IL-12 in the culture medium of the LB-, FKB-, or WCS-pulsed Jaws II cells were not observed (data not shown). These results indicated that the Jaws II cells used responded like typical myeloid-type DCs.

Stimulation of naïve T cells by *H. pylori* antigen-pulsed Jaws II cells. T-cell-proliferation assays were performed to evaluate whether clonal proliferation of T cells occurred after exposure

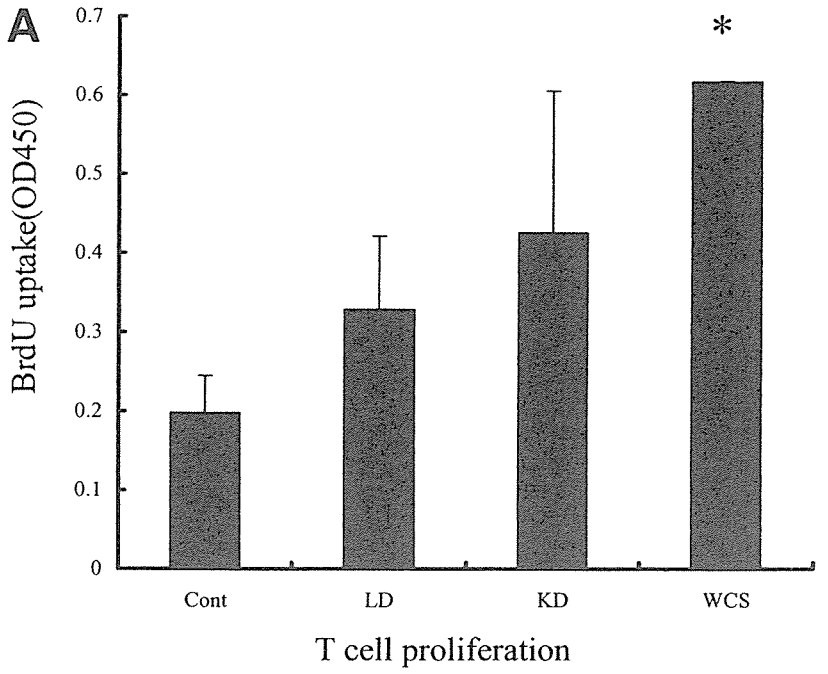
A
BrdU uptake(OD450)
0.7
0.6
0.5
0.4
0.3
0.2
0.1
0
*
Cont
LD
KD
WCS
T cell proliferation

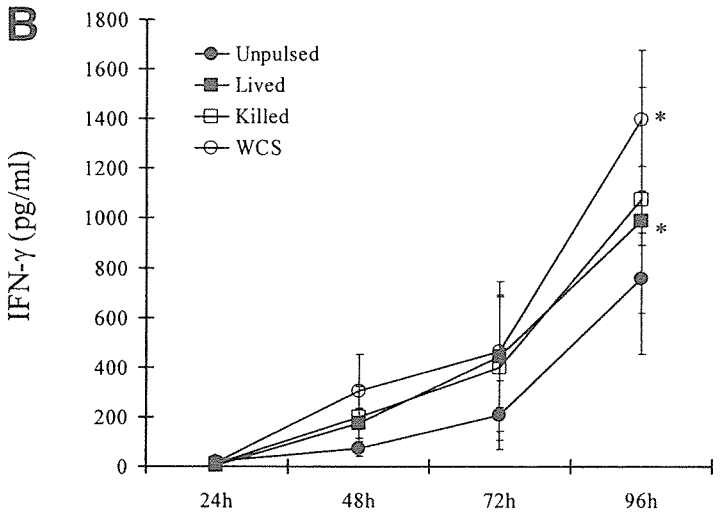
B
IFN-γ (pg/ml)
1800
1600
1400
1200
1000
800
600
400
200
0
Unpulsed
Lived
Killed
WCS
*
*
24h
48h
72h
96h

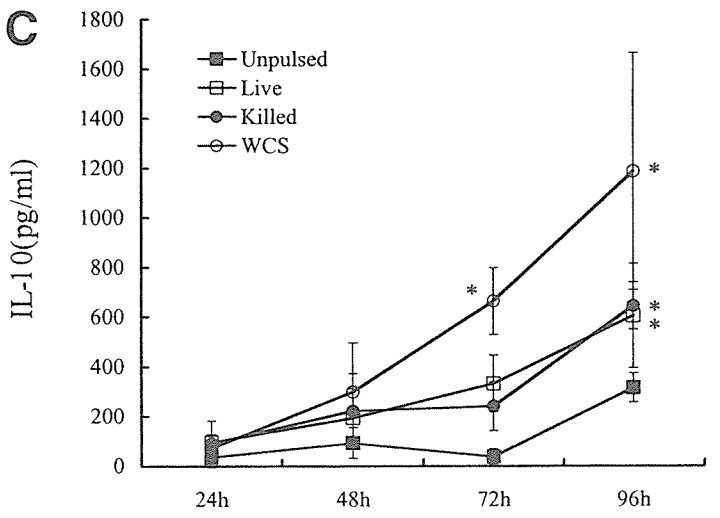
C
IL-10(pg/ml)
1800
1600
1400
1200
1000
800
600
400
200
0
Unpulsed
Live
Killed
WCS
*
*
*
*
24h
48h
72h
96h

988

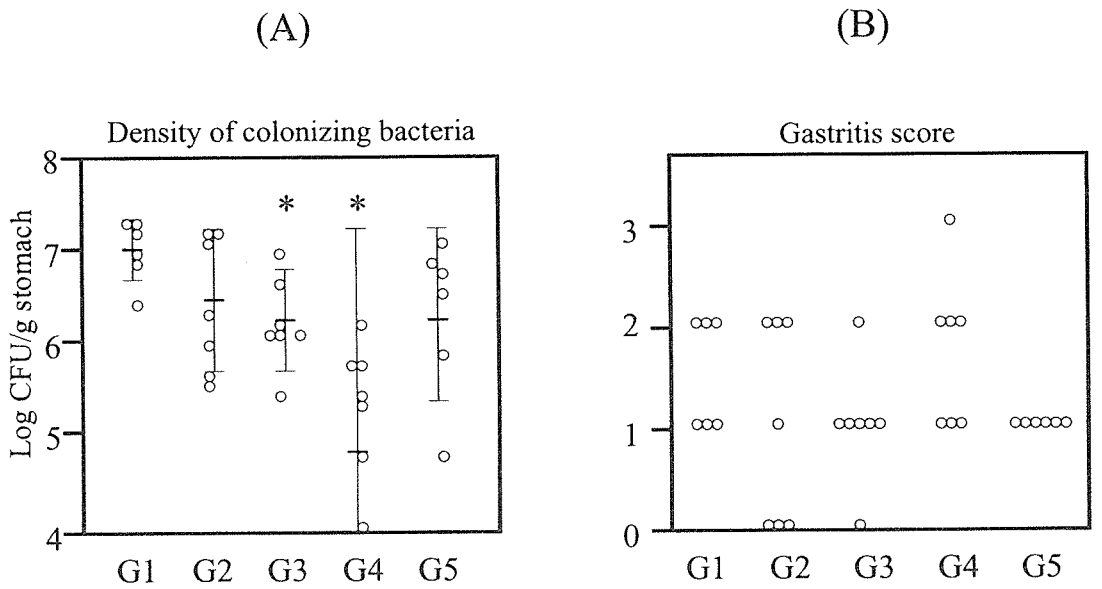

FIG. 5. C57BL/6 mice were orally inoculated with *H. pylori* strain SS1 and treated two times with the LB-pulsed (G2), the FKB-pulsed (G3), the WCS-pulsed (G4), and the unpulsed (G5) Jaws II cells, and numbers of colonizing *H. pylori* bacteria (A) and gastritis scores (B) for the mice of each group were compared to those for mice treated with PBS alone (G1). A significant reduction in the number of colonizing bacteria was observed in the G3 and G4 mice. No significant difference in gastritis scores was observed for the mice in each group. The asterisks indicate statistical significance at P of <0.05. The results are expressed as the geometric means (bold lines) ± standard deviations of results for each mouse.

to *H. pylori* antigen-pulsed Jaws II cells. The naïve-T-cell preparations were exposed to LB-, FKB-, or WCS-pulsed Jaws II cells for 48 h. The antigen-pulsed Jaws II cells were fixed with formalin prior to exposure in order to avoid possible direct interaction between the secreted cytokines and the T cells. The naïve T cells exposed to the WCS-pulsed Jaws II cells took up significantly more BrdU than the T cells exposed to the unpulsed Jaws II cells (Fig. 4A). The uptake by the T-cell groups exposed to the LB- or the FKB-pulsed Jaws II cells was greater than that by the negative control; however, the difference was not significant (Fig. 4A).

Culture media of the T cells exposed to the *H. pylori* antigen-pulsed and formalin-fixed Jaws II cells were used for the analysis of IFN-γ and IL-10 production. IFN-γ was detected at 48 h postexposure to the Jaws II cells, and the amount secreted gradually increased until 96 h postexposure. A level of IFN-γ that was significant compared to that in the negative control was observed in the culture medium of the T cells exposed to WCS- or LB-pulsed Jaws II cells at 96 h postexposure (Fig. 4B). A small amount of IL-10 was detected at 24 h postexposure to the Jaws II cells, and the amount secreted gradually increased with time (Fig. 4C). A significant amount of IL-10, compared to that in the negative control, was observed in the culture medium of the T cells exposed to the WCS-pulsed Jaws II cells at 72 h postexposure. At 96 h, T cells came to produce a significant amount of IL-10 compared to the negative control, regardless of the type of *H. pylori*-derived antigen (LB, FKB, or WCS) with which Jaws II cells were pulsed (Fig. 4C).

Therapeutic DC vaccines against *H. pylori* infection. C57BL/6 mice were orally inoculated three times with 0.5×10^8 CFU of *H. pylori* strain SS1. Approximately 1.0×10^7 CFU of bacteria per 1.0 g of stomach tissue were recovered at 3 weeks after the last inoculation in the previous study (12). Those mice were used for subsequent therapeutic DC vaccine experiments.

Mice were treated two times with the LB-pulsed (G2), the FKB-pulsed (G3), the WCS-pulsed (G4), and the unpulsed (G5) Jaws II cells, and numbers of colonizing *H. pylori* bacteria were compared to those observed when PBS was administered alone (G1). A significant reduction in the number of colonizing *H. pylori* bacteria was observed in the mice treated with the FKB-pulsed (G3) and with the WCS-pulsed (G4) Jaws II cells compared to those treated with PBS (G1) (Fig. 5A). The mean bacterial number calculated for the G4 mice was 5×10^5

FIG. 4. The naïve-T-cell preparations were exposed to Jaws II cells pulsed with LB, FKB, or WCS of *H. pylori* for 48 h at 37°C. The Jaws II cells were fixed with formalin prior to exposure. The number of Jaws II cells used was 1/20 the number of naïve T cells, and cells were exposed at 37°C for several hours. (A) Clonal proliferation of T cells was assayed by measuring the uptake of BrdU with an ELISA kit (Roche Switzerland) at 72 h postexposure. The naïve T cells exposed to the WCS-pulsed Jaws II cells showed significantly greater BrdU uptake than the others. Levels of IFN-γ (B) and IL-10 (C) production were determined using culture medium harvested at 24, 48, 72, and 96 h postexposure with separate ELISA kits (eBioscience). Significant IFN-γ production was observed in T cells exposed to WCS- or LB-pulsed Jaws II cells at 96 h. Significant IL-10 production was observed in T cells exposed to the WCS-pulsed Jaws II cells at 72 h and in T cells exposed to all *H. pylori* antigens (LB, FKB, and WCS) at 96 h postexposure. The asterisk indicates statistical significance at P of <0.05. The results are expressed as the means ± standard deviations of results for three independent cultures.

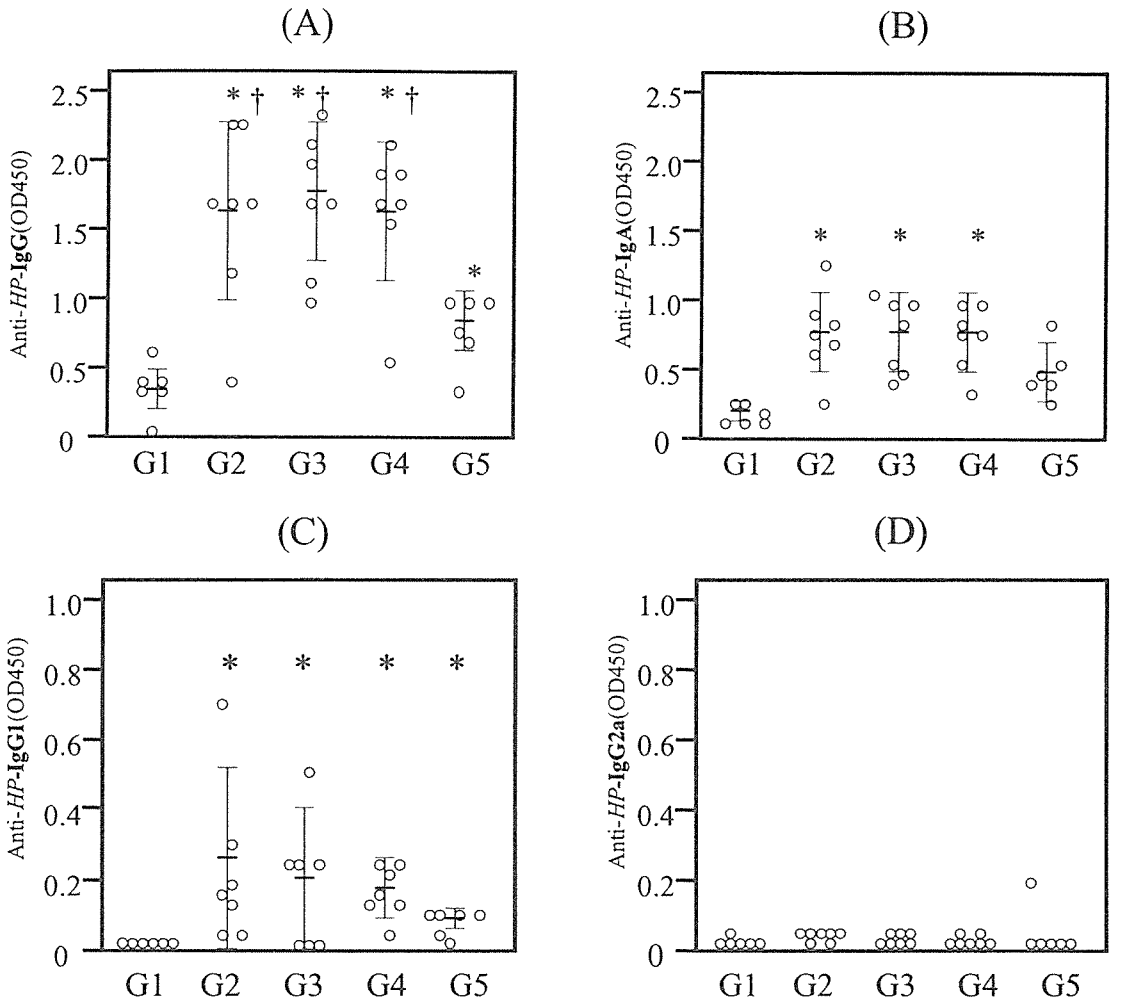

FIG. 6. Systemic humoral immune responses in mice treated with *H. pylori* antigen-pulsed Jaws II cells were evaluated. Blood samples were taken from the mice treated with the LB-pulsed (G2), the FKB-pulsed (G3), the WCS-pulsed (G4), and the unpulsed (G5) Jaws II cells, and specific antibody titers of IgG (A), IgA (B), IgG1 (C), and IgG2a (D) against *H. pylori* WCS were determined by ELISA and compared to those in mice treated with PBS (G1). Approximately 1.0 μg of *H. pylori* WCS was used to coat each well of a microtiter plate, and bound antibodies were detected using peroxidase-conjugated goat anti-mouse IgG, IgG1, IgG2a, or IgA antibody and visualized. Significant increases in IgG levels were detected in the G2, G3, and G4 mice compared to those in the G1 and G5 mice. *H. pylori*-specific IgA titers were significantly higher in the G2, G3, and G4 mice than in the G1 mice. The titer of *H. pylori*-specific IgG1 was significantly higher in G2, G3, G4, and G5 mice than in G1 mice. The titers of IgG2a in mice of all groups were below or close to the detection limit. Each sample was tested three times. The asterisks indicate statistical significance at P of <0.05. The results are expressed as the geometric means (bold lines) ± standard deviations of results for each mouse.

CFU/g of stomach tissue, which is lower by 2 logs than that obtained for the G1 mice. Gastritis scores for the mice treated with the WCS-pulsed Jaws II cells (G4) tended to be higher than those for the mice treated with PBS (G1); however, the difference was not significant (Fig. 5B).

Systemic humoral immune responses in mice treated with *H. pylori* antigen-pulsed Jaws II cells. Blood samples were collected from the mice treated with the LB-pulsed (G2), the FKB-pulsed (G3), the WCS-pulsed (G4), and the unpulsed (G5) Jaws II cells, and representative titers of antibodies against *H. pylori* WCS were compared to those in mice treated with PBS alone (G1) (Fig. 6). The antibody titers in G2, G3, and G4 mice were compared to those in G5 mice to assess the effect of antigen-pulsed Jaws II cells on the rise in specific antibody titers. Significant increases were detected in the G2, G3, G4, and G5 mice compared to the G1 mice (Fig. 6A). IgG titers were significantly higher in the G2, G3, and G4 mice than in the G5 mice (Fig. 6A). *H. pylori*-specific IgA titers were significantly higher in G2, G3, and G4 mice than in G1 mice; however, those in G5 mice were not elevated (Fig. 6B). Next, we determined titers of IgG subclasses to evaluate the status of helper-T-cell immunity. The titers of *H. pylori*-specific IgG1 were significantly higher in G2, G3, G4, and G5 mice than in G1 mice; however, the titers did not differ among the former four groups (Fig. 6C). The titers of IgG2a in mice of all groups were below or close to the detection limit (Fig. 6D).

Cytokine responses in mice treated with *H. pylori* antigen-pulsed Jaws II cells. To evaluate local cytokine responses in vivo, we determined cytokine expression levels in the gastric tissues of mice treated with the LB-pulsed (G2), the FKB-